การเสริมแรงยางธรรมชาติด้วยเถ้าลอยถ่านหินและซีโอไลท์สังเคราะห์

นางสาวเจกิตาน์ วิกรานต์วาณิชย์

วิทยานิพนธ์นี้เป็นส่วนหนึ่งของการศึกษาตามหลักสูตรปริญญาวิศวกรรมศาสตรมหาบัณฑิต
สาขาวิชาวิศวกรรมเคมี ภาควิชาวิศวกรรมเคมี
คณะวิศวกรรมศาสตร์ จุฬาลงกรณ์มหาวิทยาลัย
ปีการศึกษา 2559

REINFORCEMENT OF NATURAL RUBBER WITH COAL FLY ASH AND SYNTHETIC ZEOLITE

Miss Jaygita Wikranvanich

A Thesis Submitted in Partial Fulfillment of the Requirements

for the Degree of Master of Engineering Program in Chemical Engineering

Department of Chemical Engineering

Faculty of Engineering

Chulalongkorn University

Academic Year 2016

Thesis Title	REINFORCEMENT OF NATURAL RUBBER WITH COAL FLY ASH AND SYNTHETIC ZEOLITE
By	Miss Jaygita Wikranvanich
Field of Study	Chemical Engineering
Thesis Advisor	Associate Professor Muenduen Phisalaphong, Ph.D.

Accepted by the Faculty of Engineering, Chulalongkorn University in Partial Fulfillment of the Requirements for the Master's Degree

.....Dean of the Faculty of Engineering

(Associate Professor Supot Teachavorasinskun, Ph.D.)

THESIS COMMITTEE

.....Chairman

(Professor Bunjerd Jongsomjit, Ph.D.)

.....Thesis Advisor

(Associate Professor Muenduen Phisalaphong, Ph.D.)

.....Examiner

(Professor Artiwan Shotipruk, Ph.D.)

.....External Examiner

(Jeerun Kingkaew, Ph.D.)

เจกิตาน์ วิกรานต์วาณิชย์ : การเสริมแรงยางธรรมชาติด้วยเถ้าลอยถ่านหินและซีโอไลท์สังเคราะห์ (REINFORCEMENT OF NATURAL RUBBER WITH COAL FLY ASH AND SYNTHETIC ZEOLITE) อ.ที่ปรึกษาวิทยานิพนธ์หลัก: รศ. ดร.เหมือนเดือน พิศาลพงศ์, 62 หน้า.

ยางธรรมชาติ (NR) เป็นพอลิเมอร์ชีวภาพ ส่วนใหญ่ประกอบด้วยหน่วยย่อยของไอโซพรีน ซึ่งเป็นผลผลิตที่ได้มาจากพืช เนื่องจากคุณสมบัติที่มีความยืดหยุ่นสูง ยางธรรมชาติจึงถูกนำมาใช้กันอย่างแพร่หลายสำหรับการผลิตผลิตภัณฑ์ทางอุตสาหกรรมหลายประเภท โดยทั่วไปการเติมสารตัวเติมเข้าไปในยางธรรมชาติมีความจำเป็นสำหรับการปรับปรุงคุณสมบัติ งานวิจัยนี้จึงมุ่งเน้นไปที่การเตรียมคอมโพสิตของยางธรรมชาติโดยใช้เถ้าลอยถ่านหินและซีโอไลต์สังเคราะห์จากเถ้าลอยถ่านหินเป็นสารตัวเติม โดยมีวัตถุประสงค์ที่จะใช้ประโยชน์จากเถ้าลอยถ่านหินซึ่งเป็นกากอุตสาหกรรมมาเป็นวัตถุดิบ เพื่อเป็นการเพิ่มมูลค่าให้กับเถ้าลอยถ่านหิน รวมทั้งสามารถช่วยลดพื้นที่ที่จะต้องใช้ในการกำจัดของเถ้าลอยถ่านหินโดยการฝังกลบ นอกจากนี้ไม่เพียงแต่การเพิ่มมูลค่าของเถ้าลอยถ่านหินเท่านั้น แต่ยังสามารถปรับปรุงคุณสมบัติทางกลของคอมโพสิตยางธรรมชาติได้อีกด้วย คอมโพสิตของยางธรรมชาติถูกเตรียมโดยกระบวนการการกระจายตัวระดับอนุภาคในน้ำยาง ลักษณะทางสัณฐานวิทยาคอมโพสิตยางธรรมชาติที่มีเติม CFA, CFAT, SA และ ZA ที่ปริมาณของสารตัวเติมแตกต่างกัน ถูกวิเคราะห์ด้วยกล้องจุลทรรศน์อิเล็กตรอนไมโครสโคปแบบส่องกราด (FE-SEM) โครงสร้างทางเคมีของคอมโพสิตยางธรรมชาติถูกตรวจสอบโดยเครื่องมือวิเคราะห์สารด้วยอินฟราเรด (FT-IR) คอมโพสิตยางธรรมชาติถูกนำมาวิเคราะห์เกี่ยวกับคุณสมบัติทางกล ความเป็นผลึก ความจุของการดูดซึมน้ำและการบวมในโทลูอีน ผลที่ได้แสดงให้ว่าการเติมสารตัวเติมในปริมาณที่เหมาะสม ทำให้คุณสมบัติทางกล (มอดูลัสของยัง ความทนต่อแรงดึง และความยืดสูงสุด ณ จุดขาด) ของคอมโพสิตยางธรรมชาติดีกว่าแผ่นฟิล์มยางธรรมชาติ คอมโพสิตยางธรรมชาติโดยเฉพาะคอมโพสิตที่มีการเติมเถ้าลอยถ่านหินจะมีสมบัติความต้านทานและโครงสร้างของแผ่นฟิลม์คงทนทั้งในน้ำและโทลูอีน และเมื่อเปรียบเทียบกับยางธรรมชาติพบว่าความจุของการดูดซึมน้ำและการบวมในโทลูอีนจะลดลง อย่างไรก็ตามเนื่องจากสมบัติการชอบน้ำของสารตัวเติมทำให้ค่าความจุของการดูดซึมน้ำเพิ่มขึ้นเล็กน้อย เมื่อมีการเพิ่มปริมาณของสารตัวเติมจาก 2 ถึง 20 เทียบกับยาง 100 ส่วนโดยน้ำหนัก

ภาควิชา วิศวกรรมเคมี ลายมือชื่อนิสิต .....

สาขาวิชา วิศวกรรมเคมี ลายมือชื่อ อ.ที่ปรึกษาหลัก .....

ปีการศึกษา 2559

5770141321 : MAJOR CHEMICAL ENGINEERING

KEYWORDS: NATURAL RUBBER / COAL FLY ASH / SYNTHETIC ZEOLITE / REINFORCEMENT / COMPOSITES

JAYGITA WIKRANVANICH: REINFORCEMENT OF NATURAL RUBBER WITH COAL FLY ASH AND SYNTHETIC ZEOLITE. ADVISOR: ASSOC. PROF. MUENDUEN PHISALAPHONG, Ph.D., 62 pp.

Natural rubber (NR) is a biopolymer consisting primarily of isoprene units produced by plants. Due to its high elasticity property, NR has been widely used for manufacturing of many industrial products. Generally, the addition of fillers in NR is required for improving its properties. This work focuses on the preparation of NR composite films by using coal fly ash and synthetic zeolite from coal fly ash as filler. The objective is to exploit coal fly ash, industrial waste as a raw material for value-added products. It can also help reduce the area for disposal of coal fly ash by landfill. Moreover, this is not only to add value of coal fly ash but also the mechanical properties of the NR composite films were improved. The NR composite films were prepared via a latex aqueous micro-dispersion process. The morphology of NR composite films combing with CFA, CFAT, SA and ZA at different loading contents were characterized by field emission scanning electron microscopy (FE-SEM). The chemical structure of NR composite films were investigated Fourier Transform Infrared (FTIR) Spectroscopy. The mechanical properties, crystallinity, water absorption capacity and toluene uptake of NR composite films were analyzed. The results demonstrated that at a suitable loading range, the mechanical properties (Young's modulus, tensile strength, elongation at break) of the composite films were better than those of NR films. The composite films, especially NR-CFA also demonstrated considerably more resistance and structural stability in both water and toluene. As compared to the NR film, the WAC (water absorption capacity) and TU (toluene uptake) of the composite films were decreased. However, according to hydrophilic property of the fillers, the WAC values of the composite films were slightly increased with the increase of filler loading from 2-20 phr.

Department:	Chemical Engineering	Student's Signature	.....
Field of Study:	Chemical Engineering	Advisor's Signature	.....
Academic Year:	2016		

ACKNOWLEDGEMENTS

Firstly, I would like to express my sincere gratitude to my advisor, Associate Professor Dr. Muenduen Phisalaphong for her valuable guidance and warm encouragement throughout this research work.

I would like to acknowledge my thesis committee: Professor Dr. Bunjerd Jongsomjit, Professor Dr. Artiwan Shotipruk and Dr. Jeerun Kingkaew for their insightful comments and helpful advices for improving my work.

I am also grateful for the financial support from the Ratchadaphiseksomphot Endowment Fund of Chulalongkorn University for Postdoctoral Fellowship and the kind support of CFA from the pulping process in Prachinburi province of Thailand.

I would like to thanks all student members of Associate Professor Dr. Muenduen Phisalaphong groups as well as my friends in laboratory of Chemical Engineering Research Unit for Value Adding of Bioresources, Department of Chemical Engineering, Faculty of Engineering, Chulalongkorn University for their help, comment and friendship.

Finally, I would like to express my heartfelt thanks to my parents and my family for their support, inspiration, blessing and encouragement throughout my work and life.

CONTENTS

Page

Page

LIST OF FIGURES

LIST OF TABLES

LIST OF ABBREVIATIONS

CFA	Coal fly ash
CFAT	Coal fly ash treated by acid-washing pretreatment
NR	Natural rubber
NR-CFA	Natural rubber – Coal fly ash composites
NR-CFAT	Natural rubber – Coal fly ash treated composites
NR-SA	Natural rubber – Sodium aluminosilicate composites
NR-ZA	Natural rubber – Synthetic zeolite type A composites
Phr	Parts per hundred of rubber
SA	Sodium aluminosilicate
ZA	Synthetic zeolite type A

CHAPTER I
INTRODUCTION

1.1 Motivations

Thailand has specified its long-term energy planning in the Power Development Plan (PDP) in 2015-2036. The new plan foresees a rising use of coal and lignite, up from currently 20% to 20-25%. Therefore, the amount of coal ash was found increase followed the increasing demand for production of electricity from power plant used coal and lignite as raw material. Coal ash obtained from 5–20 wt. % of feed coal and is typically found in the form of bottom ash and fly ash, which represent 5–15 and 85–95 wt. % of the total ash generated, respectively. It was presented that Thailand generated more than 6 million tons of coal fly ash per year and elimination of coal fly ash by landfill. The disadvantages of disposal of coal fly ash are the high cost (1,500 Baht per ton) and use a lot of an area for landfill. Thus, coal fly ash was developed for utilization in many technologies. [1, 2] Coal fly ash is residues material or by-product from the combustion process of coal in power plant, which amorphous aluminosilicate. It has been used as cement additive (pozzolanic property), as backfill material, for making geopolymer binder, used as admixture for production of polymer composite, for reinforcing filler in polymers and as a precursor for synthesis of zeolites due to it has a high content of silica and alumina [3, 4]

Moreover, Thailand is the world's largest producer and exporter of natural rubber (NR) due to environment of Thailand is suitable for rubber tree growth. Thailand is able to produce a lot of rubber products such as fresh latex, solid rubber (ribbed smoked sheet, standard Thai rubber, etc.) and concentrated latex, but the price of NR tends to continuously declines owing to the oversupply in the world market. Utilization of NR for produce NR composites was studied and developed in order to enhance the value of natural rubber.

Natural rubber (NR) is an elastomeric material, high molecular weight and composed of highly cis-1, 4-polyisoprene. It has been used for manufacturing of industrial products such as glue, gloves, tires, rubber tubes, food wrap and medical products due to natural rubber is a high elasticity. However, the structure of natural rubber has an unsaturated bond or double bond. It is degraded with ultraviolet light, oxygen and ozone. Therefore, the production of natural rubber must be added of filler for preventing or improved properties. Types of fillers are used in the rubber manufacturing industry such as fly ash, silica nanoparticle, carbon black, oil palm ash, potato starch, cellulose, etc.[5-9] Preparation of NR/ filler composites has a main problem that highly aggregated and precipitated of filler in rubber matrix causes poor properties of rubber products. This problem is solved by the increase viscosity of the mixture in order to retard sedimentation and make more dispersed of filler using a thickening agent (hydrocolloid) such as alginate prior to formed NR composite films.

The aim of this work is to enhance the value of coal fly ash as industrial waste as well as to improve mechanical properties and structural stability of NR composite films by using the industrial waste. The physical and chemical properties of natural rubber composite films has been improved by using coal fly ash and synthetic zeolite derived from coal fly ash as filler via latex aqueous micro-dispersion method. The characteristics of NR composite films such as morphology, mechanical properties were investigated.

1.2 Objectives

The objective of this research is to improve mechanical and chemical properties of natural rubber composite films prepared via a latex aqueous micro-dispersion process by addition of coal fly ash and synthetic zeolite derived from coal fly ash.

1.3 Scopes of this research

1.3.1 Pretreatment of the Coal fly ash by acid-washing used hydrochloric acid to remove impurities from CFA and synthesis of zeolite using the fusion method followed by the hydrothermal method.

1.3.2 Preparation of natural rubber composite films via a latex aqueous micro-dispersion process.

1.3.3 Effects of types and contents of filler; CFA and synthetic zeolite are loading of 0, 2, 5, 8, 10, 15 and 20 phr in natural rubber composite on film properties were studied.

CHAPTER II
THEORIES AND LITERATURE REVIEWS

2.1 Coal fly ash

The coal fly ash is residues material or by-product from the combustion process of coal in power plant. It contains fine particles that is carried off in the flue gas and usually captured from the flue gas by electrostatic precipitators (ESP), baghouses, or cyclones. [10] A general flow diagram of fly ash production is presented in Figure 2.1.

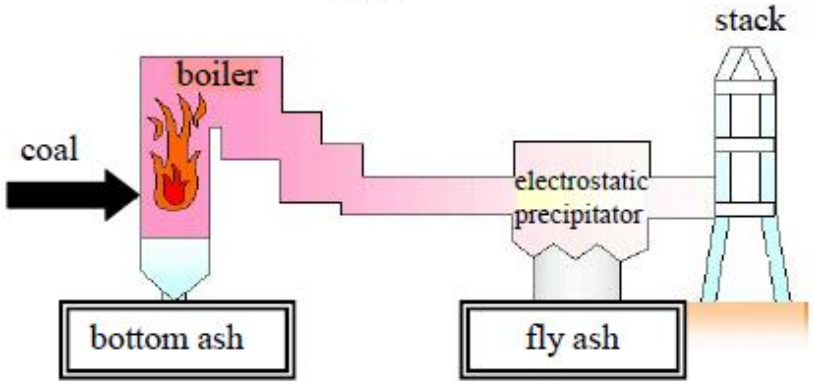

Figure 2.1 Production of coal fly ash was captured by electrostatic precipitators [7]

The coal fly ash is generally gray fine particles and major chemical components of fly ash are silicon dioxide (SiO_2), alumina (Al_2O_3), sodium oxide (Na_2O), iron oxide (Fe_2O_3) and calcium oxide (CaO). In addition, there are other impurity components such as titanium oxide (TiO_2), Magnesium oxide (MgO), Potassium oxide (K_2O). The quantity of each element depends on the source and type of coal being burned. The coal fly ash has been used as cement additive (pozzolanic property), as backfill material, for making geopolymer binder, for reinforcing filler in polymers and as a precursor for synthesis of zeolites due to it has a high content of silica and alumina.[11]

2.2 Zeolite

Zeolites are crystalline aluminosilicates, which framework structure based on silicate (SiO_4) and aluminate (AlO_4) tetrahedral linked to each other by through shared oxygen atoms (Figure 2.2). [12, 13] The zeolite synthesis procedure has two main methods, one is fusion method and the other is hydrothermal method.

Advantages of the fusion method are spending a short time in the process and producing high purity product, while the hydrothermal method has a consistent crystal pattern of zeolite product. Normally, the fusion method is preferable for the solid phase reaction and the hydrothermal method suitable for the liquid phase reaction. Raw material for zeolite synthesis has a high amount of Si and Al and impurity, therefore it was pretreated by acid washing in order to eliminating several mineral compounds prior to use in zeolite synthesis procedure. [3, 14]

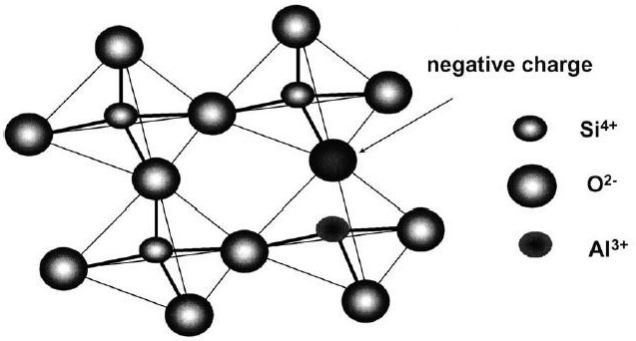

Figure 2.2 Idealized structure of zeolite framework of tetrahedral $[SiO_4]^{4-}$ with a Si/Al substitution ($[AlO_4]^{5-}$) yielding a negative charge. [14]

Common zeolite framework structures are illustrated in Figure 2.3 and Table 2.1; they have a wide variety of industrial applications such as Ion exchanger, molecular sieve or membrane for adsorption and separation (ethanol purification, flue gas; CO_2, SO_2, NO_2 treatment, purification of acid mine water), catalysts for chemical reaction (crude oil cracking, isomerization, fuel synthesis, etc.), medical, detergent, agriculture and construction.

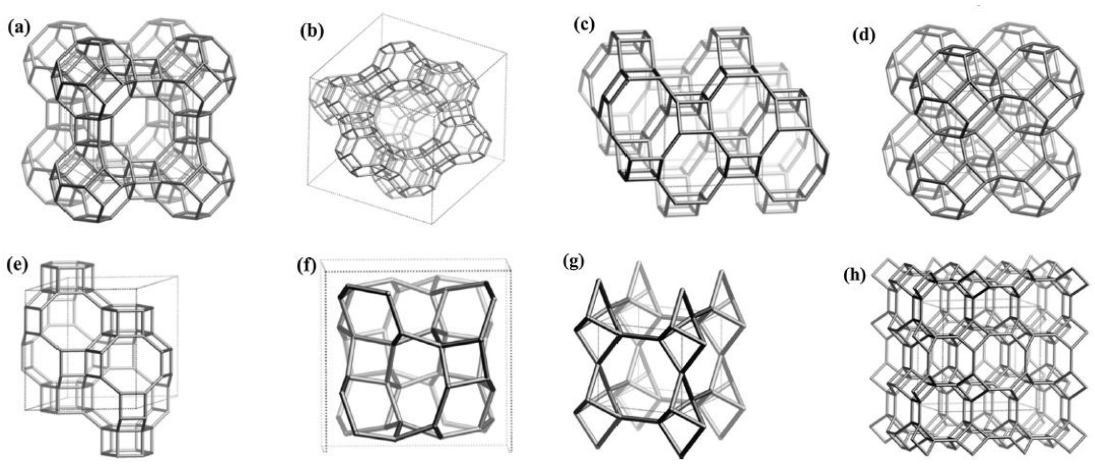

Figure 2.3 Structure of some common zeolites frameworks

(a) LTA, (b) FAU, (c) GIS, (d) SOD, (e) CHA, (f) ANA, (g) EDI and (h) MER [14]

Table 2.1 Common frameworks with their idealized cell parameters, composite building blocks (CBU) and examples of zeolites.

Framework	Idealized cell		CBU	Zeolites
	Shape	Parameters		
LTA	Cubic	a = 11.9 Å	d4r, sod, lta	Zeolite-A, SAOP-42
FAU	Cubic	a = 24.3 Å	d6r, sod	Faujasite, Na-X, Na-Y, SAPO-37, ZSM-20
GIS	Tetragonal	a = 9.8 Å, c = 10.2 Å	gis	Gismondine, Na-P, Na-P1, Na-P2, SAPO-43
SOD	Cubic	a = 9.0 Å	sod	Sodalite, hydroxysodalite, AlPO-20
CHA	Tetragonal	a = 13.7 Å, c = 14.8 Å	d6r, cha	Chabazite, AlPO-34, SAPO-34. SAPO-47
ANA	Cubic	a = 13.6 Å		Analcime, AlPO-24,
EDI	Tetragonal	a = 6.9 Å, c = 6.4 Å	nat	Edingtonite, K-F, Linde F, Zeolite N
MER	Tetragonal	a = 14.0 Å, c = 10.0 Å	dcc, d8r, pau	Merlinoite, K-M, Linde W, Zeolite W

2.3 Rubber

Rubber is an elastomer- that is one of the polymer materials and has a large variety of properties such as elasticity, strength, hardness, toughness, durability, compressibility, vibroinsulation and electrical nonconductivity. Rubber obtained from

rubber trees or chemical synthesis by polymerization reaction was it called natural rubber and synthetic rubber, respectively.

2.3.1 Natural rubber

Natural rubber (NR) has vegetable origin. It is made by enzymatic processes in plants, belonging mainly to families of Euphorbiaceae, Asteraceae (Compositae), Moraceae and Apocynaceae. Most of the commercial natural rubber is derived from the trees called *"Hevea Brazilliensis"* belonging to Euphorbiaceae family, which originates from the Amazon River in South America. Rubber trees are basically found in tropical and semitropical countries such as Indonesia, Malaysia, Vietnam, Cambodia, India, Sri Lanka, Nigeria and Brazil. [15, 16]

Natural rubber latex (NRL) refers to a white colloidal obtained from the milky secretion (latex) of the rubber plants, which contain about 30% rubber particles. The latex is concentrated by centrifugation to about 60% rubber content and added by using ammonia as a preservation of physical properties, against bacterial attack and to provide long-term stability.[17-19] Besides these also small amounts of proteins, resinous matters (including lipids) and mineral substances are shown in Table 2.2. Part of these non-rubbery matters, mainly proteins and phospholipids, is surrounded by a surface of rubbery particles that shown in Figure 2.4

Table 2.2 Composition of fresh NR latex

Constituent	Content (%)
Dry rubber content (DRC)	30 - 40
Proteins	1.0 – 1.5
Resins	1.5 – 3.0
Minerals	0.7 – 0.9
Carbohydrates	0.1 – 0.8
Water	55 – 60

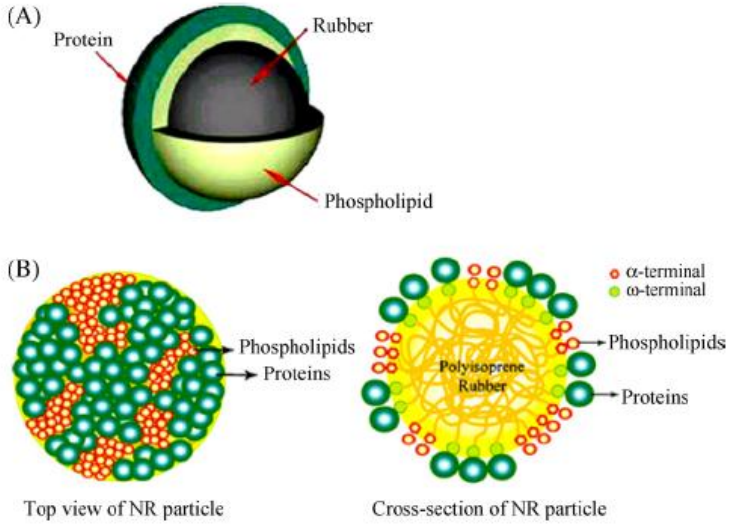

Figure 2.4 Structure of the rubber latex particle [20]

(A) Surface of rubber particle (B)Top view and cross-section of rubber particle

Natural rubber is a polymer with the chemical formula C_5H_8; it has a high molecular weight in the range of 200,000 to 500,000 daltons and composed of highly cis-1, 4-polyisoprene (Figure 2.5). The structure of natural rubber has an unsaturated bond or double bond. It's easy to react with ultraviolet light, oxygen and ozone. Therefore, the production of natural rubber must be added of filler for preventing or improved properties. [21]

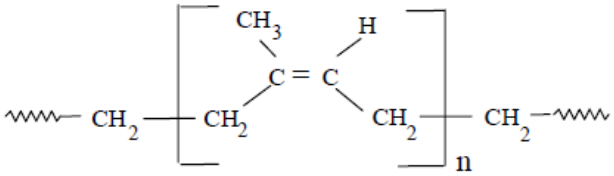

Figure 2.5 Chemical structure of cis-1,4-polyisoprene [21]

Natural rubber in form concentrated latex or solution of dry rubber is an important raw material used for manufacturing of industrial products such as glue, gloves, tires, rubber tubes, food wrap and medical products due to advantage of high elasticity of natural rubber.

2.4 Alginate

Commercial alginates are extracted primarily from the cell wall of three species of brown algae. These include *Laminaria hyperborean*, *Ascophyllum nodosum*, and *Macrocystis pyrifera*lt, in which alginate comprises almost 40% of the dry weight of these plants. Alginate is a water-soluble linear polysaccharide and is containing varying proportion of alternating blocks of 1–4 linked α-L-guluronic (G) and β-D-mannuronic acid (M) units (Figure 2.6). It is composed of homopolymeric blocks M–M or G–G, and blocks with an alternating sequence of M–G blocks that shown in Figure 2.7 [22-27]

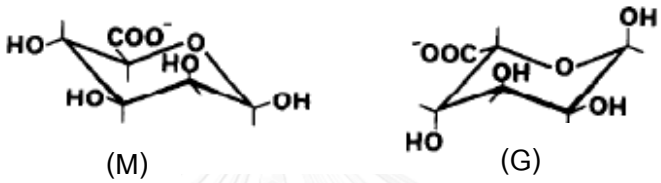

Figure 2.6 Structure of (M) β-d-mannuronic acid and (G) α-l-guluronic acid units. [26]

(A)

(B)

(C)

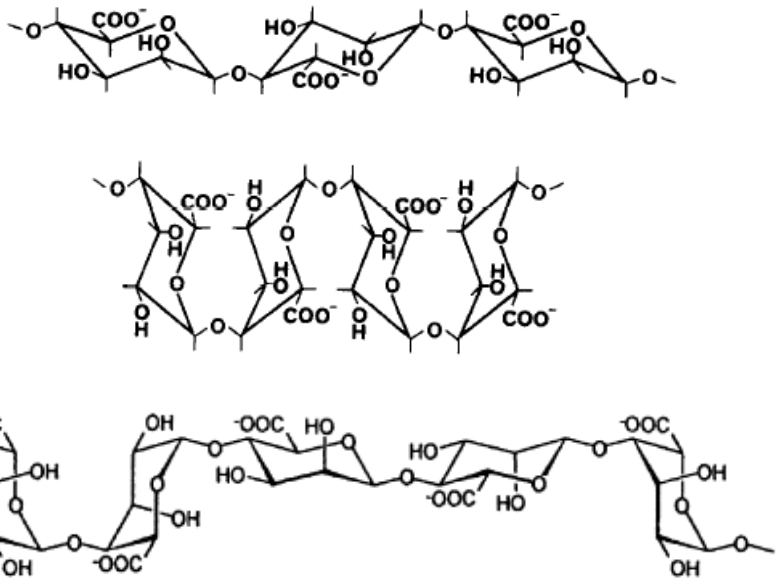

Figure 2.7 Molecular structure of sodium alginate. (A) Blocks of M; polymannuronate, (B) Blocks of G; polyguluronate (C) Blocks of random sequences [26, 27]

Alginate most important property is related to their viscosifying, stabilizing and gelling properties. Due to these properties, alginate has a broad range of applications such as thickeners, stabilizing agents and emulsifiers [28]

2.5 Improvement the properties of rubber

The improvement of rubber properties in the manufacturing industry is considered due to rubber has a wide range of properties such as elasticity, strength, hardness, toughness, durability, compressibility, therefore a several researches or study that the main aims are improvement of material properties. For example, the reinforcement process by using filler or reinforcing reagent

Cokca et al., (2004) evaluated the feasibility of utilizing rubber, fly ash and bentonite as a liner material. The mixture design consists of 90% type C fly ash and the amounts of rubber in pulverized form was waste obtained from the retreading industry, and bentonite is 0, 1, 3, 5, 7, 9 and 10% by dry weight percentages of the total mixture. The result of this study showed good properties for the construction of a liner due to hydraulic conductivity, compressibility increases as rubber percent increases and unconfined compressive strength, Young's modulus, tensile strength decreases as rubber percent increases. [5]

Peng et al., (2007) studied on preparation of natural rubber/ silica (NR/SiO_2) nanocomposite by combining self-assembly and latex-compounding techniques. The key method of this study is the encapsulation of SiO_2 nanoparticle with PDDA and NRL layers in order to improved interaction between particle-particle. Natural rubber/ silica nanocomposite films have a fixed amount of NRL with a total solid content 5% and SiO_2 loading used in this study was 0.5, 1, 2.5, 4, 6.5, 8.5 w/w. The result showed the thermal resistance and mechanical properties of nanocomposite films are improved by the SiO_2 nanoparticles are uniformly dispersed. [6]

Hasegawa et al., (2007) studied on utilization of the coal ash as filler of plastics and rubber product. The mixing composition of material is fly ash, limestone powder ($CaCO_3$) and styrene butadiene rubber (SBR). This study found that the coal ash could be used as filler like calcium carbonate due to Mooney viscosity tends to rise as amount of fly ash increases. [7]

Rattanasom et al., (2007) studied on the object of NR reinforcement with silica/ Carbon black (CB) hybrid filler at various ratios. The amount of silica or CB loading was 0, 10, 20, 30, 40 and 50 phr and the total amount of hybrid filler in each formulation was kept constant at 50 phr. For example, preparation of Silica/CB-filled NR compounds with 20 phr of silica, 30 phr of CB and the other ingredients as stearic acid, ZnO, bis(3-triethoxysilylpropyl) tetrasulfide (Si-69). The results of this study show that the vulcannizates containing 20 and 30 phr of silica in hybrid filler give the better overall mechanical properties. [8]

Ooi et al., (2013) studied the potentiality of utilizing oil palm ash (OPA) as filler in order to reinforcement of natural rubber compounds. In this study, NR compound was prepared by using low OPA loading; 0, 0.5, 1, 3, 7 and 9 phr and a semi-efficient sulphur vulcanization system was employed. The result was observed that the scorch and cure times decreased with amount OPA filled NR increases whereas maximum torque, tensile modulus and hardness increased. The rubber-filler interaction had better interfacial adhesion with the NR matrix was found 1 phr of OPA loading. [9]

Maan et al., (2014) studied making fly ash-natural rubber composite by mixing and molding process. The study was considered under the effect of two conditions; fly ash loading and particle size of fly ash (25, 75, 100 and 150 mesh). The result presented hardness, skid resistance, compression set and density are increased but tensile strength and abrasion resistance are decreased with fly ash loading increases. The particle size of fly ash had a significant effect on properties of rubber composites. It found that smaller particle size had higher hardness, tensile strength, abrasion resistance and density. [29]

Rajisha et al., (2014) studied on the preparation of natural rubber reinforcement with potato starch nanocrystal as a reinforcing agent. Potato starch nanocrystals were obtained from sulfuric acid hydrolysis of native potato starch powder prior to applying for a reinforcing agent. The content of starch was 0, 5, 10, 15 and 20 wt% mixed with NR latex at ambient temperature by using a mechanical stirrer to ensure uniform dispersion.

The nanocomposite films with uniform thickness were achieved by casting on glass mold and evaporated at 40 ºC in a ventilated oven for 4-6 h and then heated at 60 ºC under vacuum for 2 h. The mechanical properties as tensile strength and modulus were found to improve extremely with increasing nanocrystal content. [30]

Bras et al., (2010) studied on the subject of the effects of cellulose whisker loading on tensile properties, thermal properties, moisture sorption, water vapor permeation, and soil biodegradation. Cellulose whiskers from bagasse fibers were prepared by acid hydrolysis using sulfuric acid prior to use as filler in NR. The preparation of nanocomposite films was performed by reinforcing NR with various percentages of cellulose whiskers ranging from 0 to 12.5 wt%. This study was observed cellulose whiskers could be increasing the rate of biodegradation of rubber and improved of Young's modulus and tensile strength significantly when cellulose whiskers loading increased, whereas thermal properties no change in the glass transition temperature (T_g). Presence of cellulose whiskers resulted in an increase moisture sorption and decrease water vapor permeation when amount of loading increase. The optimum amount of cellulose whiskers loading for moisture sorption and water vapor permeation was 5% and 7.5%, respectively. [31]

CHAPTER III

EXPERIMENTS

3.1 Materials

Coal fly ash (CFA) used for this study was obtained from the pulping process in Prachinburi province of Thailand. Natural rubber latex (NRL) with 60% dry rubber content, high ammonia was purchased from the Rubber Research Institute of Thailand (RRIT). Hydrochloric acid (HCL), Sodium hydroxide (NaOH), Aluminum oxide (99.9% Al_2O_3 powder) and Alginate were purchased from Sigma-Aldrich.

3.2 Preparation of Coal fly ash by Acid-washing pretreatment

CFA was pretreated by 20%w/w hydrochloric acid under L/S ratio of 20 mL_{Acid}/g_{CFA}. The mixture was stirred at 80 ºC for 2 hours to remove impurities. After that, the solid sample was filtered from the acid solution and rinsed repeatedly with deionized (DI) water until the solution was neutral pH and then dried overnight at 105 ºC. The product from the pretreatment of CFA is referred as “CFAT”.

3.3 Zeolite synthesis procedure

For this part, zeolite synthesis procedure developed from Panitchakarn et al. (2014) (the fusion method followed by the hydrothermal method) was employed. Firstly, CFAT was combined with NaOH to make a NaOH/CFAT mass ratio of 2.25. Next, the mixture was burned at 550 ºC for 1 hour in furnace. After that, the product was crushed with mortar and pestle and then added into deionized water, stirred at room temperature for 12 hours. The mixture was subsequently crystallized in kiln at 80 ºC for 4 hours. Finally, the crystal was filtered from the mixture and rinsed with DI water until the filtrate was pH 10-11, then dried overnight at 105 ºC. Sodium aluminosilicate was obtained from this treatment and it was referred as “SA”. For Zeolite type A or “ZA” synthesis, the procedure is following the steps for SA synthesis, but only the Si/Al molar ratio of

CFAT was adjusted to be 1.00 by adding Al_2O_3 (Calculated from result of chemical composition analysis by X-ray fluorescence spectrometer) prior to combining with NaOH.

3.4 Preparation of natural rubber composite films

The natural rubber composite films were prepared by varying types of filler. There are four types of filler obtained from the above experiment; Coal fly ash (CFA), CFA after the pretreatment (CFAT), sodium aluminosilicate (SA) and synthetic zeolite type A (ZA). The filler loading used in this work was 0, 2, 5, 8, 10, 15 and 20 phr. Initially, the filler were thoroughly mixed with deionized water and alginate under mechanical stirring at room temperature for 30 minutes. Next, natural rubber latex (NRL) was added into the mixture. Finally, the well mixed mixture was poured into a plastic tray and dried overnight in an oven at 50 ºC to obtained natural rubber composite films. The composites of natural rubber combined with CFA, CFAT, SA and ZA are referred as NR-CFA, NR-CFAT, NR-SA and NR-ZA, respectively.

3.5 Characterization of CFA, CFAT, SA and ZA particles

CFA, CFAT, SA and ZA particles were dried and kept it in a desiccator before characterization. The overall components and particle size distribution of each dried sample were determined by X-ray fluorescence spectrometer analysis (Bruker model S8 Tiger) and Laser Particle Size Distribution Analyzer (MALVERN, Mastersizer 3000), respectively. Moreover, the morphologies of the dried samples were observed by Field emission scanning electron microscopy (FE-SEM) using a JEOL JSM-7610F (Tokyo,Japan).

3.6 Characterization of natural rubber composite films.

3.6.1 Field emission scanning electron microscopy

The morphology of the natural rubber composite films was analyzed by Field emission scanning electron microscopy (FE-SEM) using a JEOL JSM-7610F

(Tokyo,Japan) at Scientific and Technological Research Equipment Centre (STREC), Chulalongkorn University. The films of specimens were frozen in liquid nitrogen, immediately snapped, and vacuum-dried. After that, the specimens were stuck on aluminium stubs, sputtered with platinum to make electrically conductive and prevent charging on the surface. The coated specimens were kept in dry place before experiment. The FE-SEM instrument was performed at an accelerating voltage of 10 kV which was considered to be a suitable condition since too high energy can be burnt the specimens.

3.6.2 Fourier Transform Infrared (FTIR) Spectroscopy

FTIR was used to analyze about the functional groups and possible interaction between fillers and natural rubber. FTIR spectra were performed and recorded by using a Perkin-Elmer spectrum one transform Infrared Spectroscopy in the ranges of 4000-500 cm^{-1} with a resolution of 4 cm^{-1}.

3.6.3 Mechanical properties

For mechanical properties tests of dry film of NR, NR composites (Young's modulus, tensile strength, and elongation at break) were performed by using an Instron Universal testing machine (UTM) at Scientific and Technological Research Equipment Centre, Chulalongkorn University. The test conditions according to ASTM D882. At least five specimens for each different blend composition were tested.

3.6.4 X-ray diffraction (XRD)

The XRD measurements were performed on XRD diffractometer (Rigaku Miniflex II) in the 2θ range of 3–70°. The operation conditions were as follows: accelerating voltage 40 kV and electric current 30 mA. The XRD patterns of the material were taken by using a diffactometer (Bruker AXS Model D8 Discover) with Cu-Kα radiation. The XRD analyses presented structural information, crystallinity, interatomic distances and bond angles of fillers in the natural rubber composite films.

3.6.5 Water absorption capacity (WAC)

The water absorption capacity method was performed by using the specimen films with dimensions around 20×20×0.2 mm^3, and then the specimens were immersed in distilled water at room temperature. After that, the specimens were removed from water at different times and wiped with Kimwipes paper to eliminate excess water at the surface. The weight of the swollen films was measured and the procedure was repeated until there was no further weight change. At least three specimens for each different blend composition were analyzed. Water absorption capacity was calculated by using the formula:

$$\mathrm{WAC}(\%) = \left[\frac{\mathrm{W_h} - \mathrm{W_d}}{\mathrm{W_d}}\right] \times 100$$

Where, $\mathrm{W_h}$ and $\mathrm{W_d}$ are the weights of the specimen hydrated and dried, respectively.

3.6.6 Toluene uptake (TU)

The NR and NR composite films were prepared with dimensions around 20×20×0.2 mm3. Next, the specimens were immersed in toluene at room temperature. After that, the weight of the swollen films was weighed and the procedure was repeated until there was no further weight change. The toluene uptake was calculated by using the formula:

$$\mathrm{TU}(\%) = \left[\frac{\mathrm{W_t} - \mathrm{W_0}}{\mathrm{W_0}}\right] \times 100$$

Where, $\mathrm{W_0}$ and W_t are the weights of the specimen before swelling and after a time (t) of immersion, respectively

CHAPTER IV

RESULTS AND DISCUSSION

4.1 Characterization of CFA, CFAT, SA and ZA particles

4.1.1 X-ray fluorescence spectrometer (XRF) analysis

The chemical composition analysis of CFA, CFAT, SA and ZA samples were performed by wavelength dispersive x-ray fluorescence spectrometry was reported in Table 4.1. The major components of the original CFA were silica as silicon oxides about 52.6%, alumina as aluminium oxides about 28.5% and the impurities consisted of metallic oxides such as Fe and Ca. Other components were presented in small amounts included MgO, K_2O and TiO_2. Moreover, the results show that most of the impurities (Fe_2O_3, CaO, and other impurities) in CFA can be eliminated by acid-washing pretreatment. These results consistent with Sarode D. B., et al. [32] and Shivpuri et al. [33] who presented that heavy metals from coal fly ash showed a high leachability in acidic or ion-exchangeable conditions. The main constituents of SA and ZA were composed of SiO_2, Al_2O_3 and Na_2O, whereas the Si/ Al molar ratio of SA and ZA as 1.84 and 1.09, respectively.

4.1.2 Particle size distribution

The particle size distribution of CFA and CFAT present in a range of 0.5 to 200 μm with a maximum between 30 to 40 μm as shown in Figure 4.1(a) and 4.1(b), whereas the particle size distribution of SA and ZA present in a range of 0.5 to 100 μm with a maximum between 20 to 30 μm and 3 to 4 μm, respectively as shown in Figure 4.1(c) and 4.1(d). From the particle size distribution curve of ZA in Figure 4.1(d) shows a bimodal distribution with the mean particle sizes about 3 μm and 25 μm The zeolite synthesis is a long time process and during the synthesis, the formation of zeolite nuclei (Nucleation) can occur together with the accumulation of zeolite crystals (crystallization) [34]. Therefore, the sizes of the ZA particles could be diverted.

4.1.3 Field emission scanning electron microscopy (FESEM)

The morphology of CFA, CFAT (3,000X, 5.00 kV) and SA, ZA particles (10,000X, 2.00 kV) are shown in Figure 4.2(A), 4.2(B), 4.2(C) and 4.2(D), respectively. CFA and CFAT particles are composed of spherical particles and irregular unshaped fragments. SA particles are unshaped and not shown spherical or crystal, whereas ZA particles displayed the presence of crystal with the cubic morphology. From the FESEM images, crystalline phase of CFA, CFAT and SA was not detected, which could indicate that CFA, CFAT and SA were amorphous materials.

Table 4.1 Chemical compositions of CFA, CFAT, SA and ZA samples

Chemical composition	CFA (%wt)	CFAT (%wt)	SA (%wt)	ZA (%wt)
SiO_2	52.6	61.4	46.3	33.7
Al_2O_3	28.5	23.4	25.2	30.9
Na_2O	0.396	0.315	16.7	18.4
Fe_2O_3	10.8	2.80	3.31	1.27
CaO	2.63	0.567	0.678	0.303
MgO	1.51	0.828	0.827	0.487
K_2O	1.11	1.05	0.330	0.189
TiO_2	1.03	0.996	1.29	0.509
SO_3	0.973	0.116	105 ppm	125 ppm
P_2O_5	0.151	700 ppm	-	-
V_2O_5	367 ppm	-	-	-

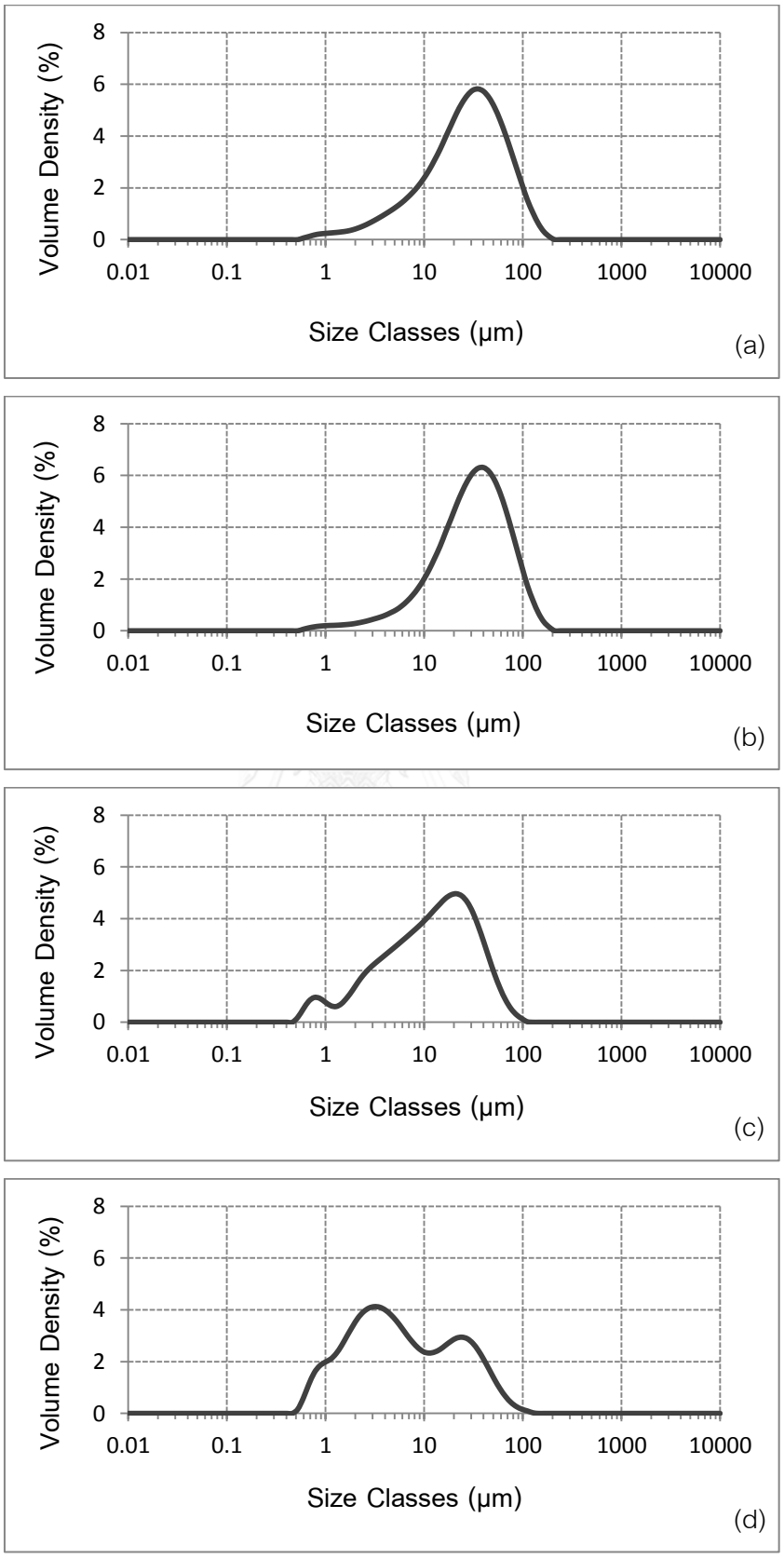

Figure 4.1 Particle size distribution of CFA (a), CFAT (b), SA (c), ZA (d) particles.

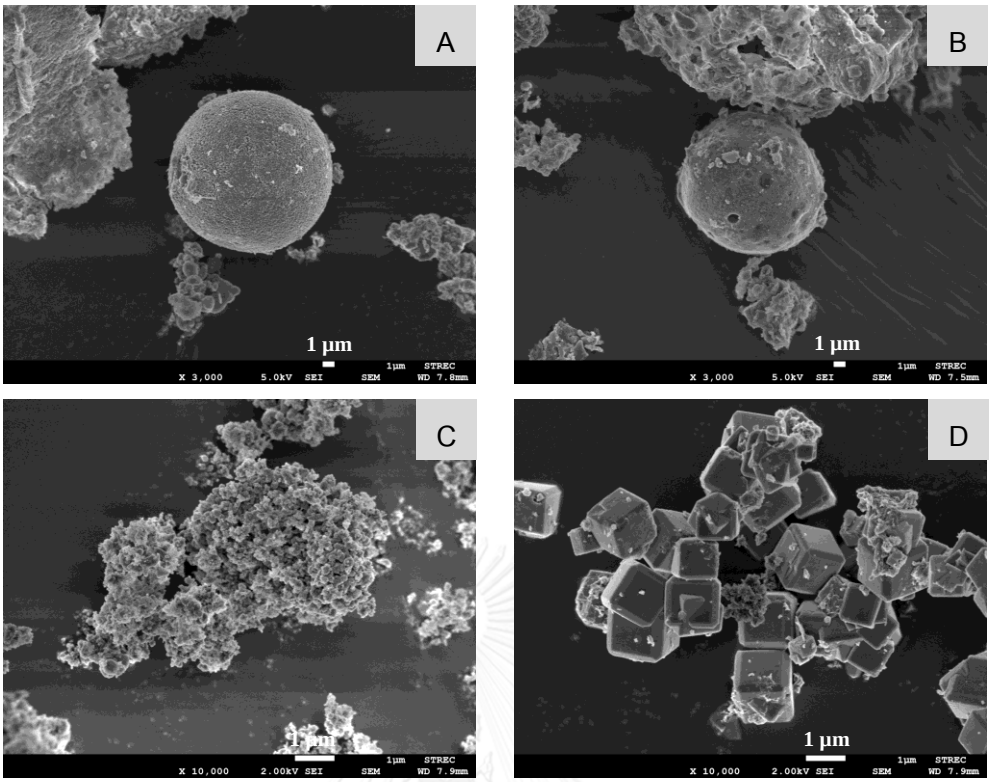

Figure 4.2 FESEM micrographs of CFA (A), CFAT (B), SA (C), ZA (D) particles.

4.2 Characterization of NR, NR-CFA, NR-CFAT, NR-SA and NR-ZA films

4.2.1 Field emission scanning electron microscopy (FESEM)

The surface and cross-section morphologies of NR were analyzed by FESEM as shown in Figure 4.3. The NR film has a smooth and glossy surface. From the cross-section view, the thickness of NR film was about 400 µm. Some fractures on the cross section were observed owing to input force to break the film apart after the immersion in liquid nitrogen.

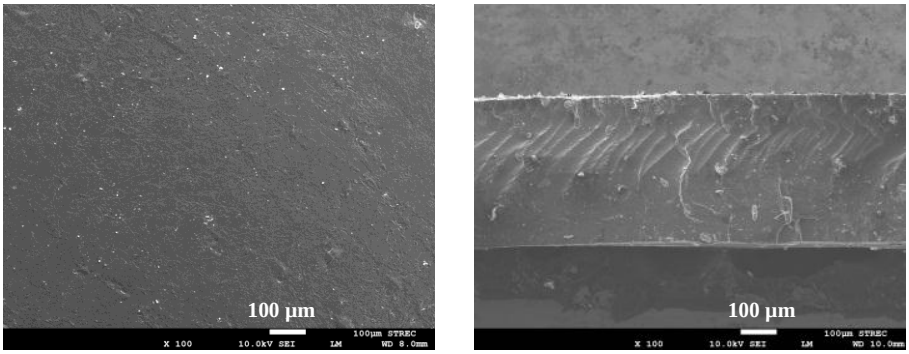

Figure 4.3 FESEM micrographs of surface and cross-section morphologies of NR

The NR composite film samples were formed by loading of CFA, CFAT, SA and ZA at 5, 10 and 20 phr. The morphologies of the composites and dispersion of each filler in NR matrix by FESEM are shown in Figure 4.4 and 4.5.

Figure 4.4 shows the surface morphologies of NR composite film samples at different type and loading of fillers: NR-CFA (Figure 4.4A-C), NR-CFAT (Figure 4.4D-F), NR-SA (Figure 4.4G-I) and NR-ZA (Figure 4.4J-L). The micrographs show that NR composite film samples have a rough surface. The roughness increased when the loading content of filler increased. The cross-section morphologies of NR-CFA, NR-CFAT, NR-SA and NR-ZA composite films at 5, 10 and 20 phr viewed at a magnification of 500X are shown in Figure 4.5A-C, Figure 4.5D-F, Figure 4.5G-I and Figure 4.5J-L,respectively. It was demonstrated that filler particles were uniformly dispersed on the surface (shown in Figure 4.4) and within the NR matrix (shown in Figure 4.5) without phase separation.

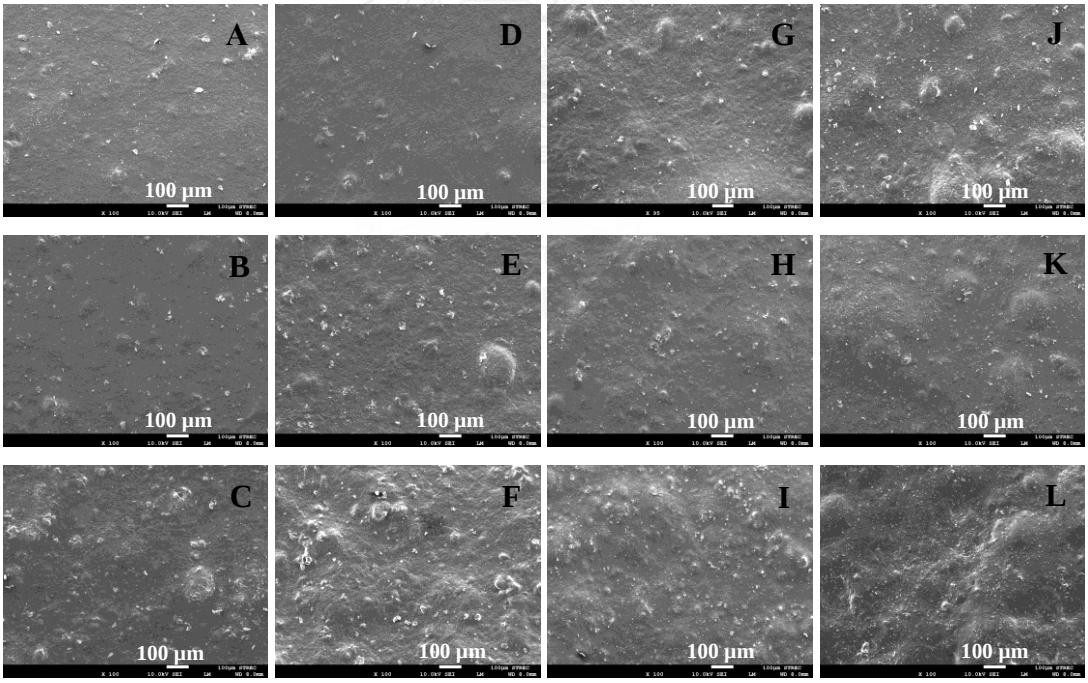

Figure 4.4 FESEM micrographs of surface morphologies of NR composite films: (A) NR-CFA5, (B) NR-CFA10, (C) NR-CFA20, (D) NR-CFAT5, (E) NR-CFAT10, (F) NR-CFAT20, (G) NR-SA5, (H) NR-SA10, (I) NR-SA20, (J) NR-ZA5, (K) NR-ZA10, (L) NR-ZA20

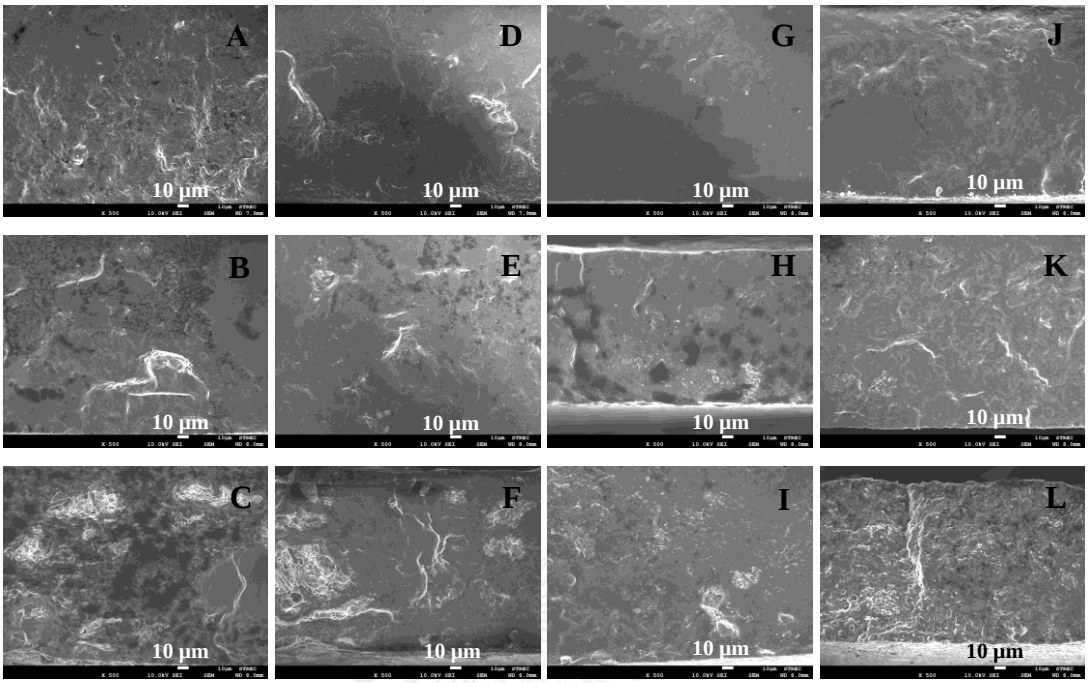

Figure 4.5 FESEM micrographs of cross-section morphologies of NR composite films: (A) NR-CFA5, (B) NR-CFA10, (C) NR-CFA20, (D) NR-CFAT5, (E) NR-CFAT10, (F) NR-CFAT20, (G) NR-SA5, (H) NR-SA10, (I) NR-SA20, (J) NR-ZA5, (K) NR-ZA10, (L) NR-ZA20

4.2.2 Fourier Transform Infrared (FTIR) Spectroscopy

The FTIR of NR, CFA, CFAT, SA, ZA and NR composite films with different type and various loading of filler were presented in Figure 4.6, 4.7, 4.8 and 4.9, respectively. Pure NR spectra adsorbed at 2916 and 2853 cm^{-1} are assigned to asymmetric stretching vibration of methyl ($-CH_3$). In addition, it is appeared a peak of symmetric stretching vibration of methylene ($-CH_2$) at 2960 cm^{-1}. The C=C stretching is situated at 1660 cm^{-1} and OH–stretching at 3291 cm^{-1}. The FTIR spectra of the CFA and CFAT reveal a peak of OH– stretching at 3435 cm^{-1} and asymmetric stretching of Si-OH bending at 1628 cm^{-1}. The peak at 1088 $cm^{-1}$is due to asymmetric stretching vibration of Si-O. The Al/Si-O bending vibration is observed at the peak symmetric stretching at 798 cm^{-1}.The quartz bending vibration is also observed at 779 cm^{-1}. The results show that the CFA and CFAT sample has a high amount of Si and Al which agree to the XRF results reported by Panitchakarn et al.[3]. Pure SA has a peak of asymmetric stretching at 1004 cm^{-1}, symmetric stretching at 710 cm^{-1} and asymmetric stretching of

Si-OH bending at 1642 cm^{-1}, whereas Pure ZA has a peak of asymmetric stretching vibrations of bridge bonds Si-O at 1004 cm^{-1}. The symmetric stretching vibrations of bridge bonds Si-O-Al is observed at 666 cm^{-1} and symmetric stretching vibrations of bridge bonds Si-O-Si and bending vibrations O-Si-O (complex band) at 555 cm^{-1}. The isolated OH– stretching is situated at 3434-3435 cm^{-1}. The FTIR spectra of Pure ZA is consistent with Mozgawa et al. [35] and Douglas et al. [36].

The FTIR spectra of NR-CFA, NR-CFAT, NR-SA and NR-ZX composite films show peaks at 3301-3316 cm^{-1}, 2961 cm^{-1}, 2914-2915 cm^{-1} and 1607-1610 cm^{-1}, which are assigned to OH, $-CH_2$, $-CH_3$ and C=C stretching, respectively. The position of characteristic peaks of composites slightly shifted from peaks of reactants, which might imply some weak interactions without chemical reaction between NR and fillers.

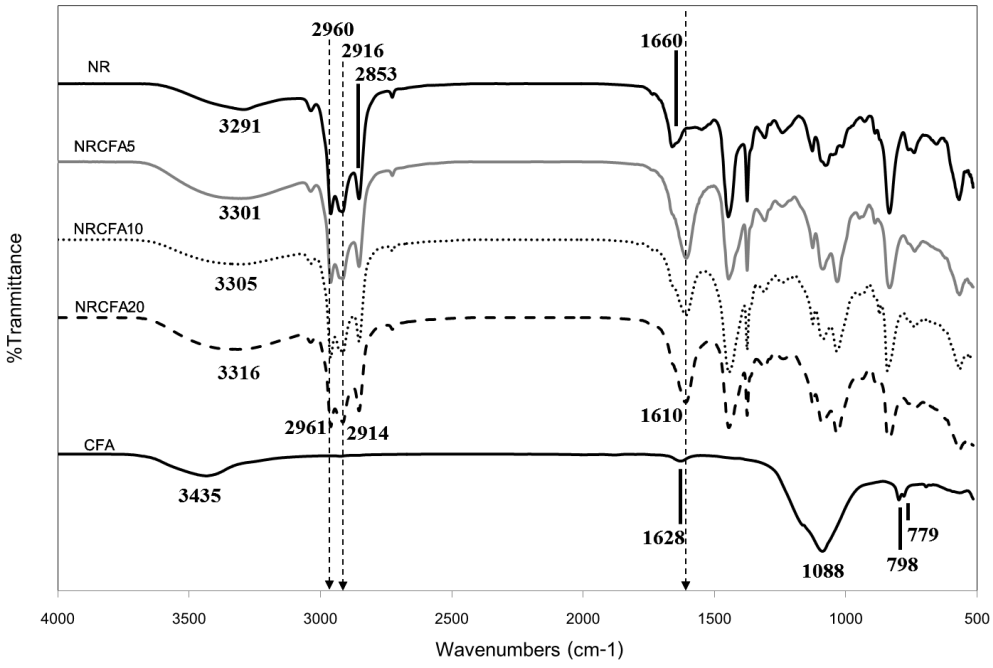

Figure 4.6 FTIR of the NR, CFA and NR-CFA composite films

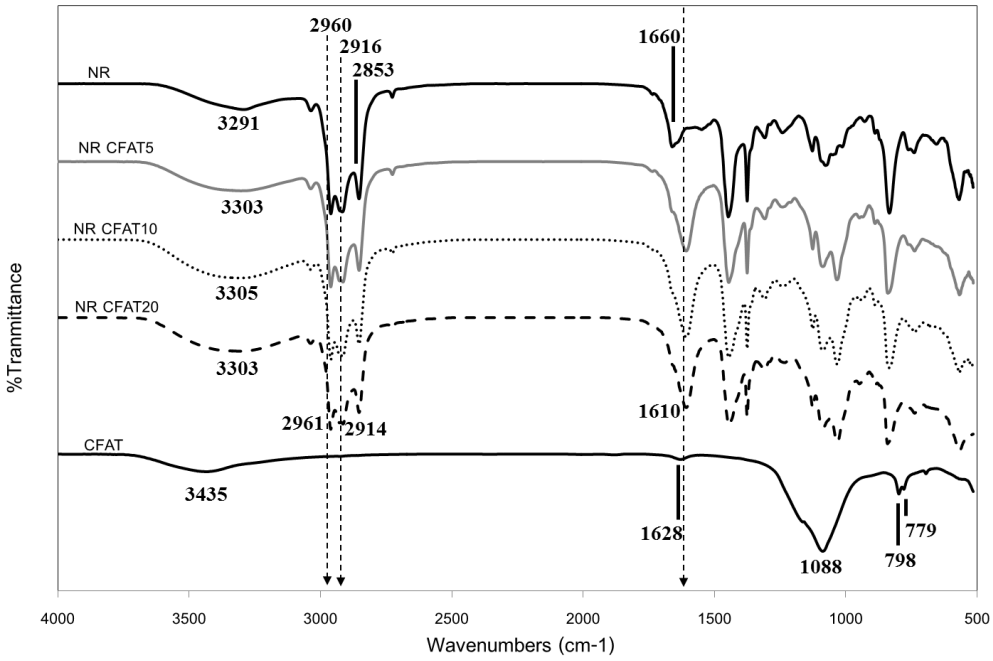

Figure 4.7 FTIR of the NR, CFAT and NR-CFAT composite films

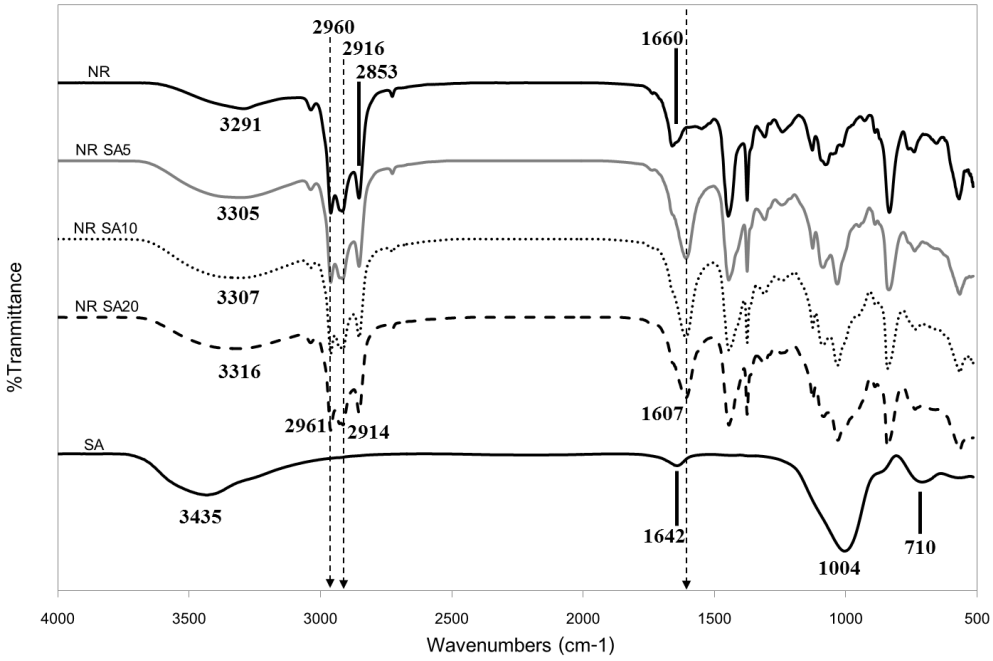

Figure 4.8 FTIR of the NR, SA and NR-SA composite films

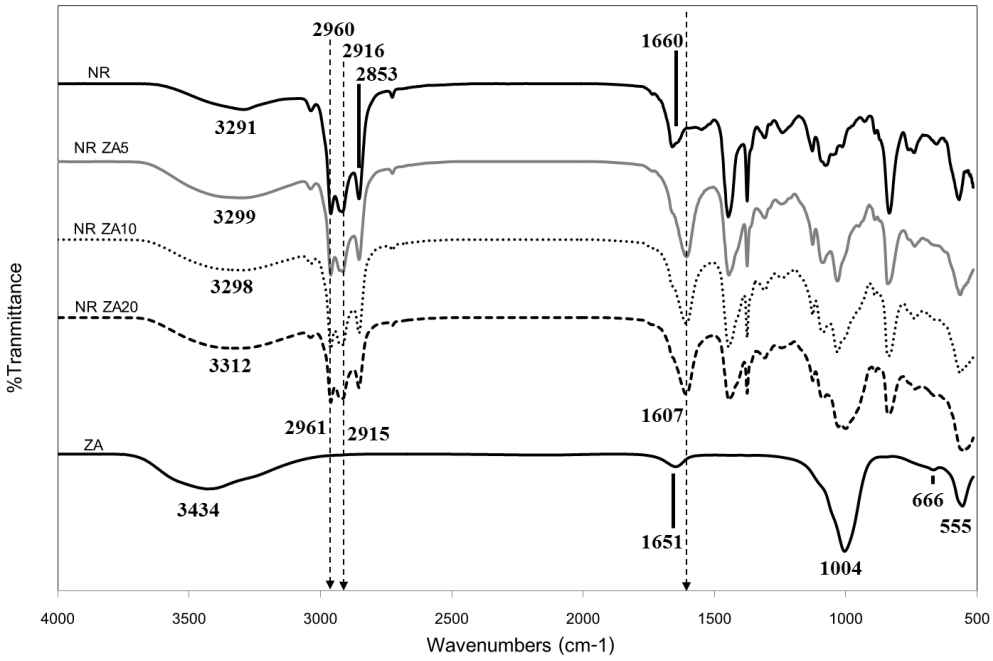

Figure 4.9 FTIR of the NR, ZA and NR-ZA composite films

4.2.3 Mechanical properties

The Mechanical properties of NR, NR-CFA, NR-CFAT, NR-SA and NR-ZA composite films were analyzed as shown in Figure 4.10. Thin film of pure NR has young's modulus, tensile strength and elongation at break of 2.4 MPa, 1.2 MPa and 99.4%, respectively. The mechanical properties of pure NR were significantly improved by reinforcement with CFA, CFAT, SA and ZA. With CFA, CFAT, SA and ZA loading at 20 phr, the values of Young's modulus of composite films were increased to 125.9, 21.4, 4.4 and 4.9 MPa, respectively (Figure 4.10A). The CFA loading showed considering more effect on the Young's modulus of NR-CFA composite as compared to the other NR composites and the Young's modulus increased with the increased loading of CFA. Some increase of the Young's modulus was observed with the loading of CFAT 2 to 20 phr. The loading contents of SA and ZA at less than 20 phr, shows no significant effect on the Young's modulus of the NR-SA and NR-ZA. However, the values of Young's modulus were found increased to about 2 times with SA and ZA loading at 20 phr.

The tensile strength of the NR-CFA, NR-CFAT, NR-SA and NR-ZA films increased to about 6-10 times of the NR film as shown in Figure 4.10B. The tensile strength increased with increasing filler loading. The maximum tensile strength of NR-CFA and NR-CFAT was observed at 10.5 and 7.7 Mpa with loading at 20 phr. Moreover, the optimal tensile strength of NR-SA and NR-ZA was observed at 14.3 and 11.8 Mpa with loading at 15 phr. However, when the amount of SA and ZA are added in NR matrix more than 15 phr, the values of tensile strength of NR composite films are slightly decreased due to agglomeration of fillers.

The values of elongation at break of NR composite films are shown in Figure 4.10C. Form the result, the highest elongation at break of NR-CFA and NR-ZA was observed at 290.7% and 515.3% with CFA and ZA loading at 10 phr, respectively. However, the highest elongations at break of NR-CFAT and NR-SA were observed at 318.7 and 510.0 with the filer loading at 15 and 5 phr, respectively.

From this result, it was demonstrated that SA and ZA were more efficient to be used as filler to increase tensile strength and elongation at break of NR composite film more than CFA and CFAT, whereas CFA and CFAT were more efficient to use for improvement of the Young's modulus of the NR composite films more than SA and ZA.

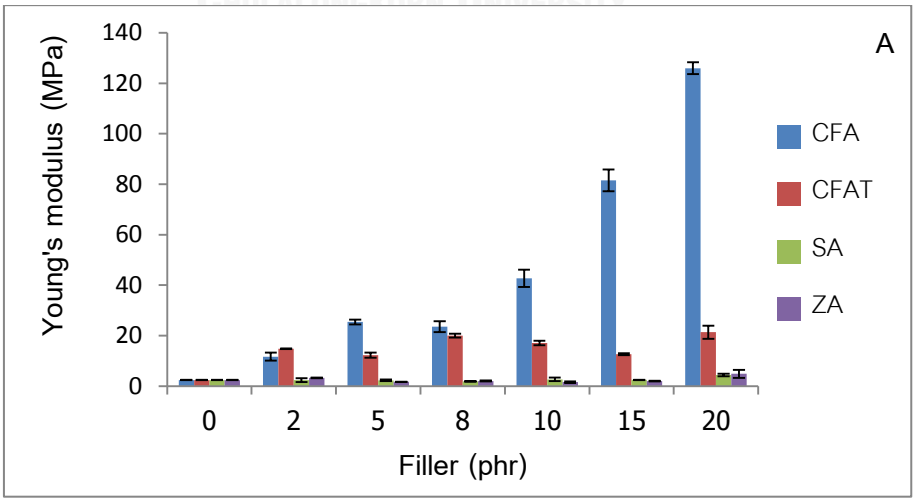

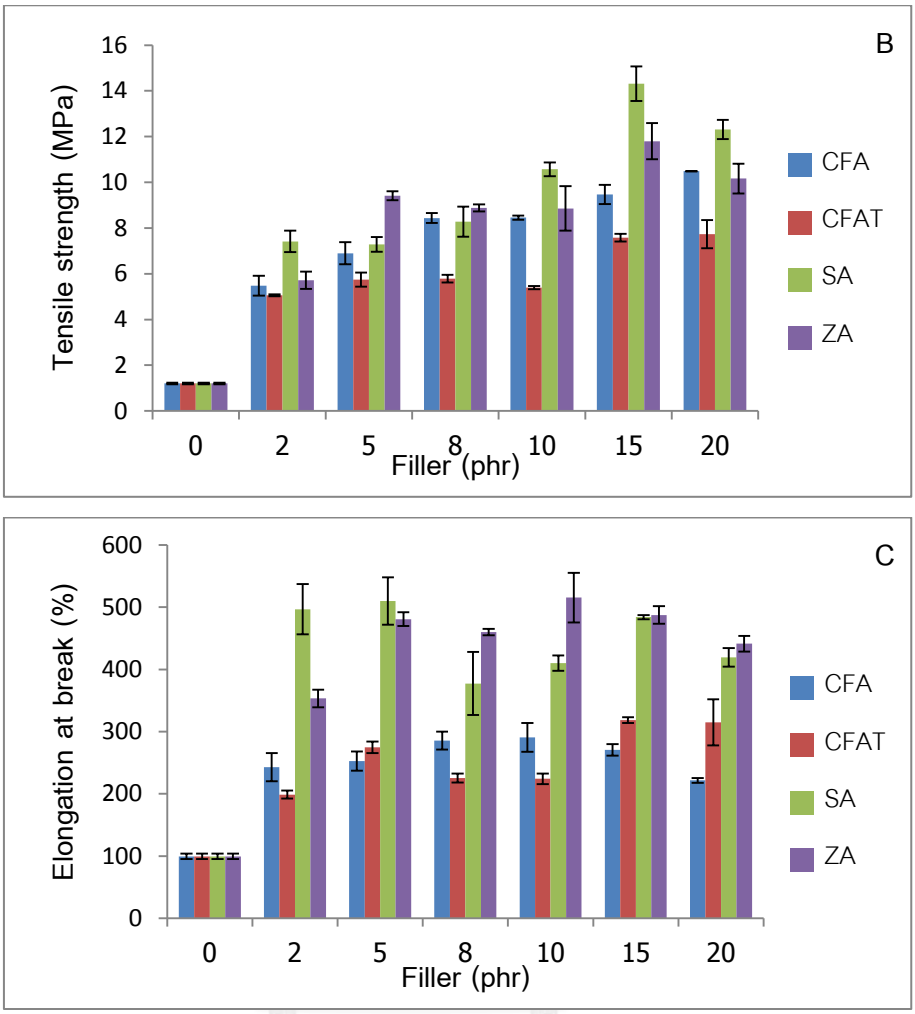

Figure 4.10 Mechanical properties of NR, NR-CFA, NR-CFAT, NR-SA and NR-ZA composite films with different filler loading content.

4.2.4 X-ray diffraction (XRD)

The XRD patterns of NR and NR composite film samples with CFA, CFAT, SA and ZA loading at 0, 5, 10 and 20 phr are shown in Figure 4.11A to D. The CFA and CFAT presented amorphous phase. The shape XPD peaks at 21.6 and 26.6 degrees 2θ present quartz crystal. The SA in Figure 4.11C was amorphous sodium aluminosilicate zeolite due to quartz phase was completely decomposed, whereas XRD patters of ZA in Figure 4.11C was presented crystalline phase in the formation of Zeolite type A. These results concur well with the previous reports [3, 37-39]. Moreover, the diffraction peak intensity of the NR composite film increased with loading content of

CFA, CFAT, and ZA increased. It was demonstrated that NR composite film had a better crystallinity than NR film.

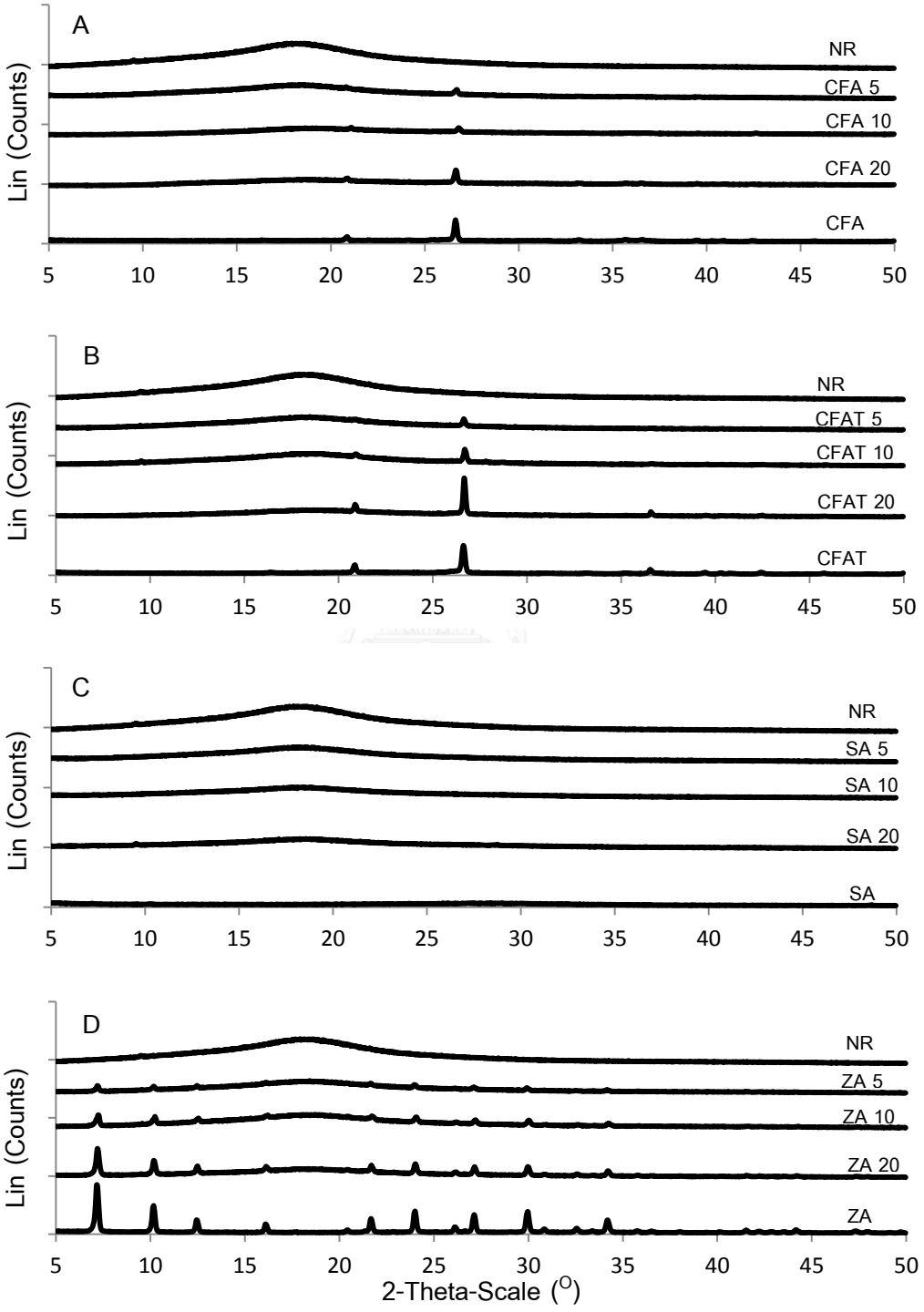

Figure 4.11 X-ray diffraction of the composite films with the loaded content of CFA (A), CFAT (B), SA (C) and ZA (D) at 0, 5, 10 and 20 phr

4.2.5 Water absorption capacity (WAC)

Figure 4.12 to 4.15 show the water absorption capacity of NR, NR-CFA, NR-CFAT, NR-SA and NR-ZA, which were plotted as a function of time. The study of WAC of specimens with filler loading at 0, 2, 5, 8, 10, 15 and 20 phr were carried out. It was clearly shown that the modified NR films by adding fillers derived from CFA had more resistance in water. NR film had considerably higher WAC and low structural stability in water than those of the NR composite films. The swelling behavior of NR and NR composite films are shown in Figure A.1-4. However, the WAC of the composite films relatively increased with increasing the amount of CFA, CFAT, SA and ZA, respectively. It could be described that the polarity and hydrophilic of filler particles within the NR matrix could affect WAC of the NR composite film. This observation is consistent with the previous report by Maan et al.[29]. Among all NR-composites in this study, WAC of NR-CFA films had lower WAC as compared to the others. The degrees of WAC were in order: NR-ZA>NR-SA>NR-CFAT>NR-CFA. It took about 7 days for NR-CFA and 2 days for NR-CFA, NR-SA and NR-ZA to adsorb water and reach its adsorption equilibrium. Overall, NR-ZA has the highest water resistance due to it absorbed less water and has better structural stability in water than the other NR composites in this study.

4.2.6 Toluene uptake (TU)

The toluene uptake studies of NR, NR-CFA, NR-CFAT, NR-SA and NR-ZA composite films with different filler contents were carried out by the immersion of the films in toluene at room temperature for 8 h as shown in Figure 4.16 to 4.19. The results show that the toluene uptake of NR film increased to maximum absorption value at 3223% in 2 h. After 2 h, it was decreased due to NR film dissolved in toluene. While the toluene uptake of NR composite film modified by fillers derived from CFA in this study rapidly increased in 1 h and then reached to the plateau period (equilibrium). However, the toluene uptake decreased with increasing the amount of CFA, CFAT, SA and ZA. It can be described that filler particles could not absorb toluene (non-polar solvent) due to the major components of fillers (SiO_2 and Al_2O_3) are polar molecules. Furthermore, the

swelling behavior of NR and NR composite films in toluene are in Figure A.5-8. It was demonstrated that the structural stability of NR composite film in toluene (as nonpolar solvent) was noticeably improved with the addition of fillers (CFA and fillers derived from CFA). After NR-CFA films were immersed in toluene for 8 h, the film remained flat with slightly swelling (Figure A.5), whereas NR-SA and NR-ZA films significantly swelled and were in a rolling shape after 8 h of the immersion in toluene(Figure A.7 and Figure A.8). NR-CFAT has the least resistance of all NR composites in this study; it was decomposed into small pieces after the immersion in toluene for 4 h (Figure A.6).

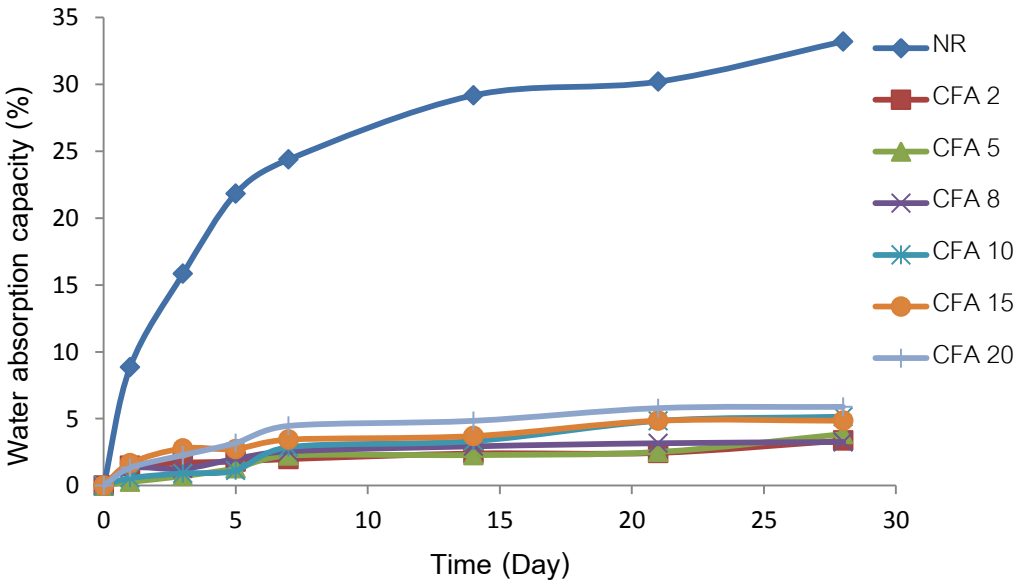

Figure 4.12 Water absorption capacity (%) of NR and NR-CFA composite films

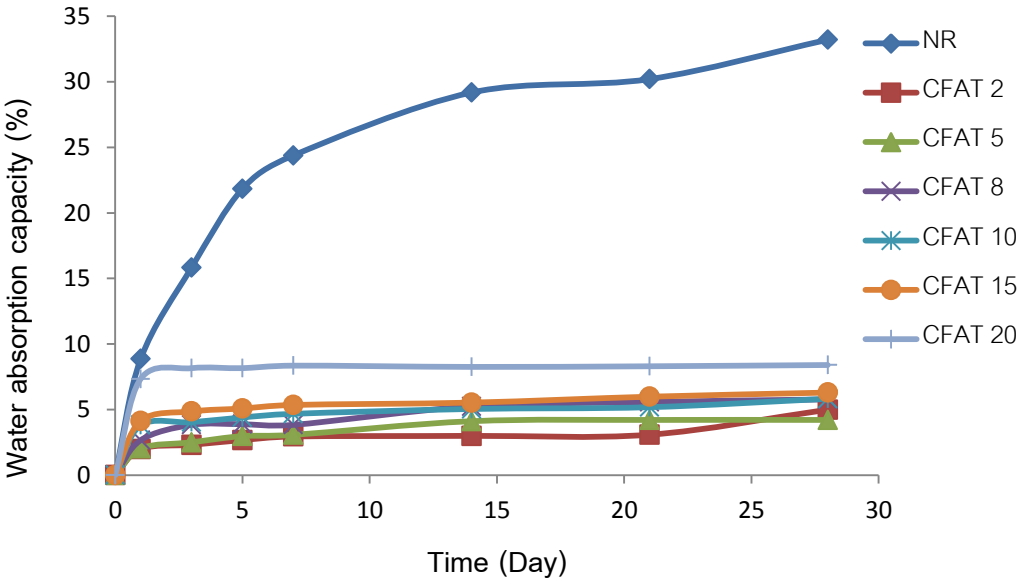

Figure 4.13 Water absorption capacity (%) of NR and NR-CFAT composite films

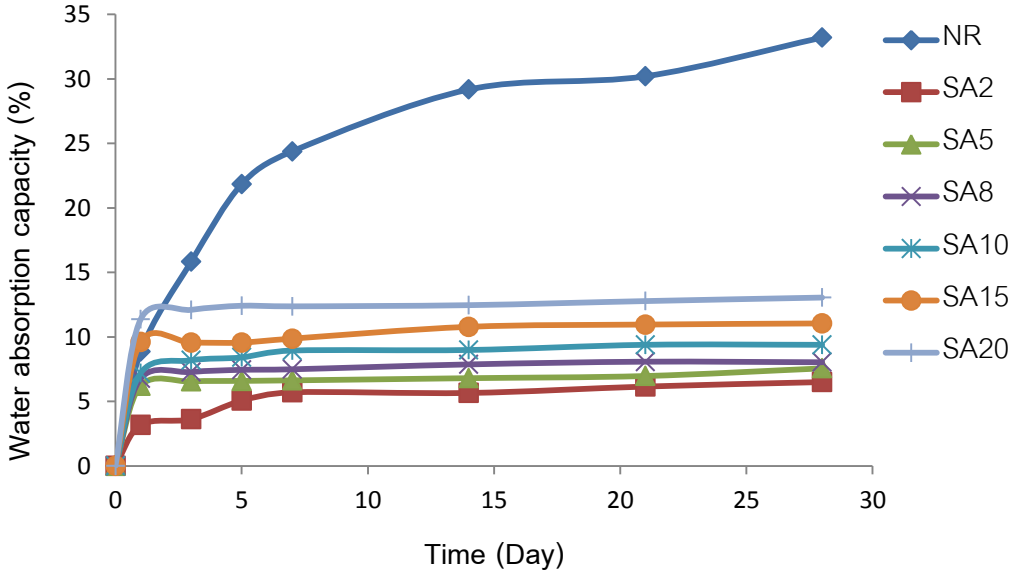

Figure 4.14 Water absorption capacity (%) of NR and NR-SA composite films

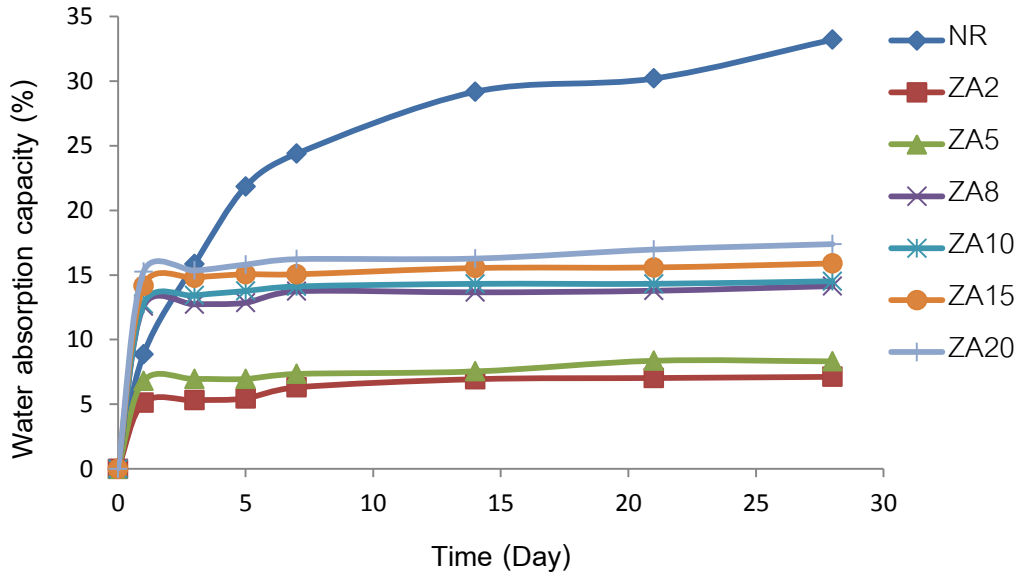

Figure 4.15 Water absorption capacity (%) of NR and NR-ZA composite films

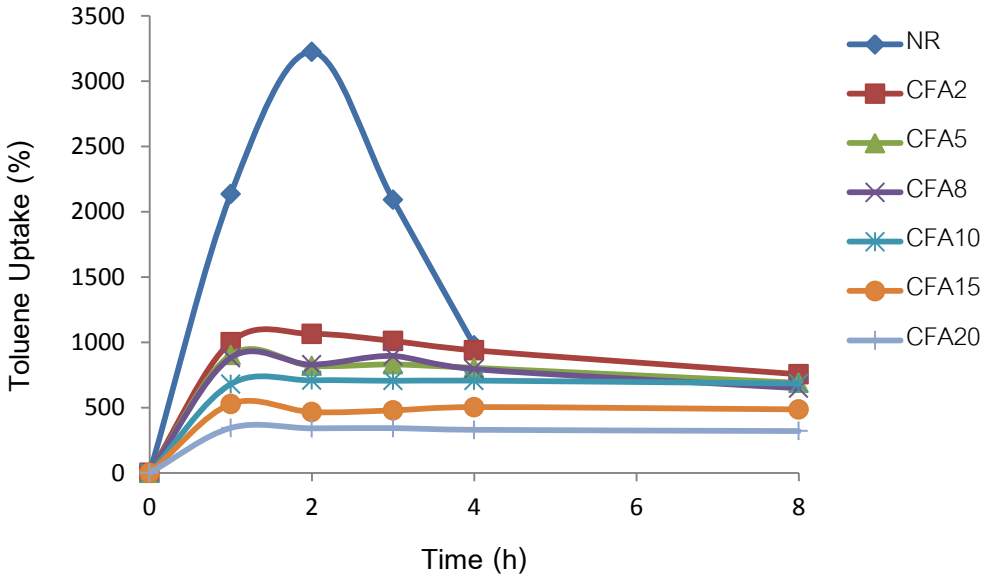

Figure 4.16 Toluene uptake (%) of NR and NR-CFA composite films

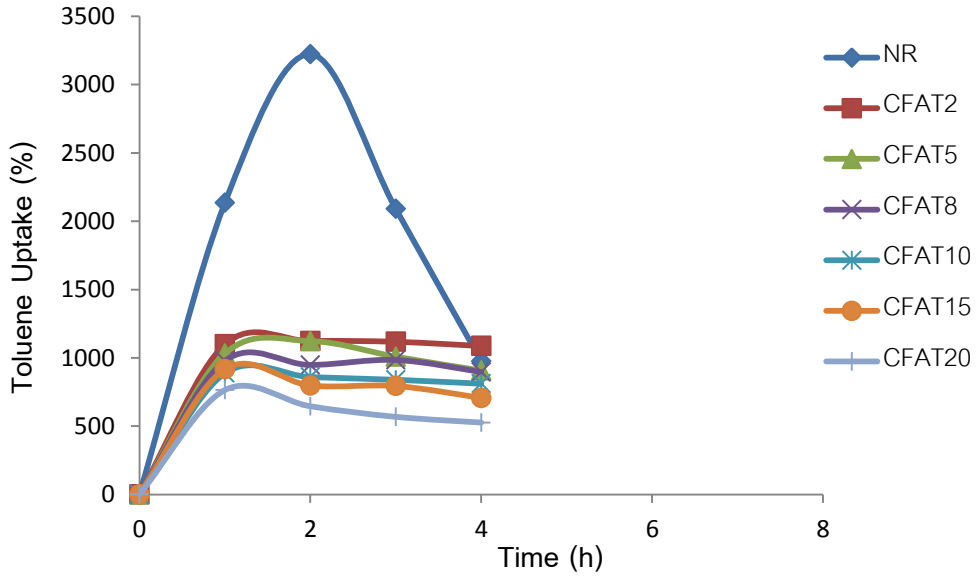

Figure 4.17 Toluene uptake (%) of NR and NR-CFAT composite films

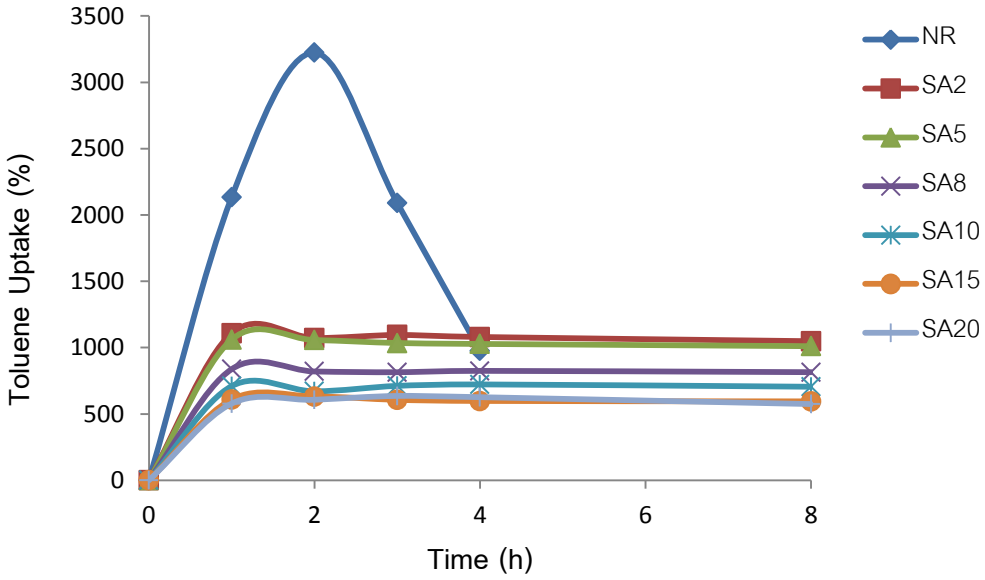

Figure 4.18 Toluene uptake (%) of NR and NR-SA composite films

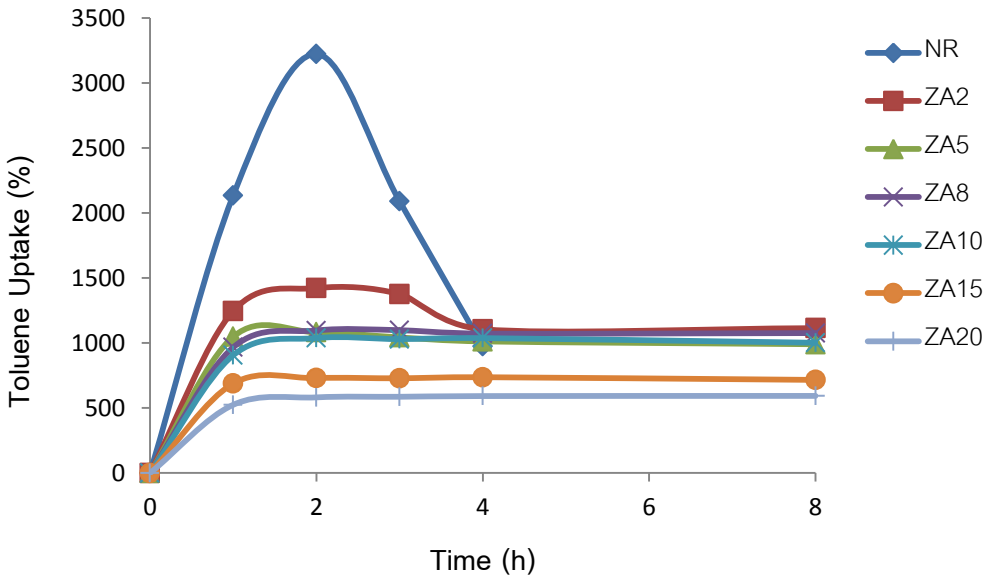

Figure 4.19 Toluene uptake (%) of NR and NR-ZA composite films

CHAPTER V
CONCLUSIONS

The NR-CFA, NR-CFAT, NR-SA and NR-ZA composite films with filler loading at 2, 5, 8, 10, 15 and 20 phr were successfully fabricated via a latex aqueous micro-dispersion process. The morphology studies of these composites films from FESEM show that CFA, CFAT, SA and ZA particles were well distributed and dispersed in NR matrix. Some weak interactions between filler and NR were observed by FTIR analysis. The mechanical and chemical properties of NR composites films were improved by reinforcement with CFA, CFAT, SA and ZA. Young's modulus, tensile strength, elongation at break and crystallinity of the NR-filler composite films are increased. The composite films also demonstrated significantly more resistance and structural stability in both water and toluene. As compared to the NR film, the WAC (water absorption capacity) and TU (toluene uptake) of the composite films were decreased. The NR-CFA films show the highest improvement in Young's modulus and have the highest structural stability and resistance in both toluene and water. The composites of NR-SA and NR-ZA show the highest improvement in tensile strength and elongation at break. The properties of the composites films significantly depend on the type and loading amount of the filers.

REFERENCES

[1] Yao ZT, Ji XS, Sarker PK, Tang JH, Ge LQ, Xia MS, et al. A comprehensive review on the applications of coal fly ash. Earth-Science Reviews. 2015;141:105-21.

[2] Office EPaP. Thailand Power Development Plan (PDP: 2015-2036). In: Ministry of Energy T, editor. http://www.eppo.go.th/power/PDP2015/PDP2015.pdf.

[3] Panitchakarn P, Laosiripojana N, Viriya-umpikul N, Pavasant P. Synthesis of high-purity Na-A and Na-X zeolite from coal fly ash. Journal of the Air & Waste Management Association. 2014;64:586-96.

[4] Ruen-ngam D, Rungsuk D, Apiratikul R, Pavasant P. Zeolite Formation from Coal Fly Ash and Its Adsorption Potential. Journal of the Air & Waste Management Association. 2009;59:1140-7.

[5] Cokca E, Yilmaz Z. Use of rubber and bentonite added fly ash as a liner material. Waste Management. 2004;24:153-64.

[6] Peng Z, Kong LX, Li S-D, Chen Y, Huang MF. Self-assembled natural rubber/silica nanocomposites: Its preparation and characterization. Composites Science and Technology. 2007;67:3130-9.

[7] Hasegawa M, Furukawa S, Asana M. Utilization of the Coal Ash as Filler of Plastics and Rubber Products. Proceedings of International Symposium on EcoTopia Science. 2007:842-5.

[8] Rattanasom N, Saowapark T, Deeprasertkul C. Reinforcement of natural rubber with silica/carbon black hybrid filler. Polymer Testing. 2007;26:369-77.

[9] Ooi ZX, Ismail H, Abu Bakar A. Synergistic effect of oil palm ash filled natural rubber compound at low filler loading. Polymer Testing. 2013;32:38-44.

[10] Wongsa A, Zaetang Y, Sata V, Chindaprasirt P. Properties of lightweight fly ash geopolymer concrete containing bottom ash as aggregates. Construction and Building Materials. 2016;111:637-43.

[11] Koshy N, Singh DN. Fly ash zeolites for water treatment applications. Journal of Environmental Chemical Engineering. 2016;4:1460-72.

[12] Visa M. Synthesis and characterization of new zeolite materials obtained from fly ash for heavy metals removal in advanced wastewater treatment. Powder Technology. 2016;294:338-47.

[13] Bukhari SS, Behin J, Kazemian H, Rohani S. Conversion of coal fly ash to zeolite utilizing microwave and ultrasound energies: A review. Fuel. 2015;140:250-66.

[14] Querol X, Moreno N, Umaña JC, Alastuey A, Hernández E, López-Soler A, et al. Synthesis of zeolites from coal fly ash: an overview. International Journal of Coal Geology. 2002;50:413-23.

[15] Berthelot K, Lecomte S, Estevez Y, Peruch F. Hevea brasiliensis REF (Hev b 1) and SRPP (Hev b 3): An overview on rubber particle proteins. Biochimie. 2014;106:1-9.

[16] Mariano M, El Kissi N, Dufresne A. Cellulose nanocrystal reinforced oxidized natural rubber nanocomposites. Carbohydrate polymers. 2016;137:174-83.

[17] Wang S, Liu J, Wu Y, You Y, He J, Zhang J, et al. Micromorphological characterization and label-free quantitation of small rubber particle protein in natural rubber latex. Analytical biochemistry. 2016;499:34-42.

[18] Ali Shah A, Hasan F, Shah Z, Kanwal N, Zeb S. Biodegradation of natural and synthetic rubbers: A review. International Biodeterioration & Biodegradation. 2013;83:145-57.

[19] Rippel MM, Lee L-T, Leite CAP, Galembeck F. Skim and cream natural rubber particles: colloidal properties, coalescence and film formation. Journal of Colloid and Interface Science. 2003;268:330-40.

[20] Nawamawat K, Sakdapipanich JT, Ho CC, Ma Y, Song J, Vancso JG. Surface nanostructure of Hevea brasiliensis natural rubber latex particles. Colloids and Surfaces A: Physicochemical and Engineering Aspects. 2011;390:157-66.

[21] Kajornchaikul W. Rubber Products: Manufacturing & Technology. The Thailand Research Fund (TRF). 2557;3:204.

[22] George M, Abraham TE. Polyionic hydrocolloids for the intestinal delivery of protein drugs: alginate and chitosan--a review. Journal of controlled release : official journal of the Controlled Release Society. 2006;114:1-14.

[23] Nussinovitch A, Dagan O. Hydrocolloid liquid-core capsules for the removal of heavy-metal cations from water. Journal of hazardous materials. 2015;299:122-31.

[24] Liew CV, Chan LW, Ching AL, Heng PW. Evaluation of sodium alginate as drug release modifier in matrix tablets. International journal of pharmaceutics. 2006;309:25-37.

[25] Thu HE, Zulfakar MH, Ng SF. Alginate based bilayer hydrocolloid films as potential slow-release modern wound dressing. International journal of pharmaceutics. 2012;434:375-83.

[26] GACESA P. Enzymic degradation of alginates. Inl J Biochem. 1992;24(4):545-52.

[27] Yang J, Zhao J, Fang Y. Calorimetric studies of the interaction between sodium alginate and sodium dodecyl sulfate in dilute solutions at different pH values. Carbohydrate research. 2008;343:719-25.

[28] Mazur K, Buchner R, Bonn M, Hunger J. Hydration of Sodium Alginate in Aqueous Solution. Macromolecules. 2014;47:771-6.

[29] Maan A, Niyogi UK, Singh AK, Mehra DS, Rattan S. Development and Characterization of Fly Ash Reinforced Natural Rubber Composite. Journal of Polymer Materials. 2014;31:397-408.

[30] Rajisha KR, Maria HJ, Pothan LA, Ahmad Z, Thomas S. Preparation and characterization of potato starch nanocrystal reinforced natural rubber nanocomposites. International journal of biological macromolecules. 2014;67:147-53.

[31] Bras J, Hassan ML, Bruzesse C, Hassan EA, El-Wakil NA, Dufresne A. Mechanical, barrier, and biodegradability properties of bagasse cellulose whiskers reinforced natural rubber nanocomposites. Industrial Crops and Products. 2010;32:627-33.

[32] Sarode DB, Jadhav RN, Khatik VA, Ingle ST, Attarde SB. Extraction and Leaching of Heavy Metals from Thermal Power Plant Fly Ash and Its Admixtures. Polish Journal of Environmental Studies 2010;19:1325-30.

[33] Shivpuri KK, B L, Kulkarni DA, Dikshit AK. Metal Leaching Potential in Coal Fly Ash. American Journal of Environmental Engineering. 2012;1:21-7.

[34] Cundy CS, Cox PA. The hydrothermal synthesis of zeolites: Precursors, intermediates and reaction mechanism. Microporous and Mesoporous Materials. 2005;82:1-78.

[35] MOZGAWA W, KRÓL M, BARCZYK K. FT-IR studies of zeolites from different structural groups. CHEMIK. 2011;65:667-74.

[36] Douglas S, Cheamsawat N, Hussaro K. Synthesis of Zeolite A from Aluminium Etching By-product. The 2nd Joint International Conference on “Sustainable Energy and Environment (SEE 2006).1-5.

[37] Alves Fungaro D, Valério da Silva M. Utilization of Water Treatment Plant Sludge and Coal Fly Ash in Brick Manufacturing. American Journal of Environmental Protection. 2014;2:83-8.

[38] Alves JABLR, Dantas ERS, Pergher SBC, Melo DMA, Melo MAF. Synthesis of high value-added zeolitic materials using glass powder residue as a silica source. Materials Research. 2014;17:213-8.

[39] Lee K-M, Jo Y-M. Synthesis of zeolite from waste fly ash for adsorption of CO2. Journal of Material Cycles and Waste Management. 2010;12:212-9.

APPENDIX

Table A.1 Data for Figure 4.10

Samples	Modulus (MPa)		Tensile (MPa)		Elongation (%)	
	Average	SD	Average	SD	Average	SD
NR	2.446	0.0964	1.203	0.0299	99.4	4.3822
NRCFA2	11.697	1.5824	5.475	0.4341	242.8	22.7476
NRCFA5	25.423	0.9439	6.897	0.4844	252.7	15.5200
NRCFA8	23.553	2.1285	8.440	0.2234	285.4	14.4431
NRCFA10	42.763	3.4118	8.457	0.0907	290.7	23.1805
NRCFA15	81.500	4.2930	9.470	0.4162	270.7	9.4170
NRCFA20	125.967	2.3180	10.487	0.0058	221.5	3.9051
NRCFAT2	14.853	0.1222	5.060	0.0361	198.7	6.3791
NRCFAT5	12.283	0.9905	5.743	0.3092	274.6	9.1799
NRCFAT8	20.040	0.7817	5.787	0.1677	225.2	7.2858
NRCFAT10	17.103	0.9352	5.397	0.0709	224.2	8.5196
NRCFAT15	12.697	0.3710	7.580	0.1709	318.7	4.6188
NRCFAT20	21.383	2.6045	7.733	0.6096	314.7	37.1251
NRSA2	2.413	0.7761	7.413	0.4697	496.7	40.5134
NRSA5	2.314	0.3707	7.287	0.3265	510.0	38.0000
NRSA8	1.895	0.0889	8.280	0.6580	377.3	50.7674
NRSA10	2.699	0.6965	10.573	0.3011	410.0	12.4900
NRSA15	2.456	0.0717	14.313	0.7550	484.0	3.4641
NRSA20	4.444	0.4879	12.310	0.4194	419.3	15.1438
NRZA2	3.261	0.1747	5.720	0.3816	353.3	14.0475
NRZA5	1.700	0.0252	9.413	0.1914	480.7	11.0151
NRZA8	2.057	0.2165	8.883	0.1570	460.0	5.2915
NRZA10	1.581	0.2839	8.860	0.9728	515.3	40.0666
NRZA15	2.025	0.1316	11.797	0.7925	487.3	14.1892
NRZA20	4.866	1.6359	10.167	0.6506	441.3	12.7017

(SD: Standard deviation)

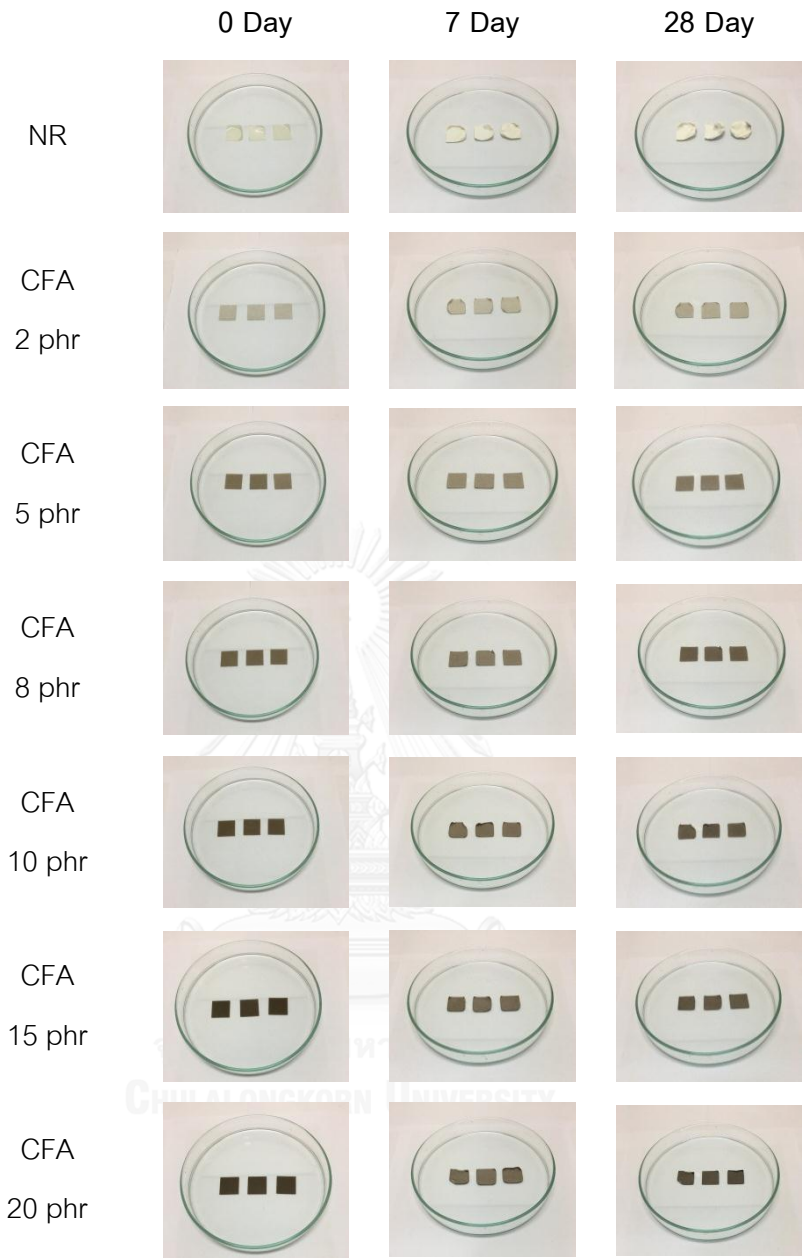

Figure A.1 The swelling behavior in water of NR-CFA composite films.

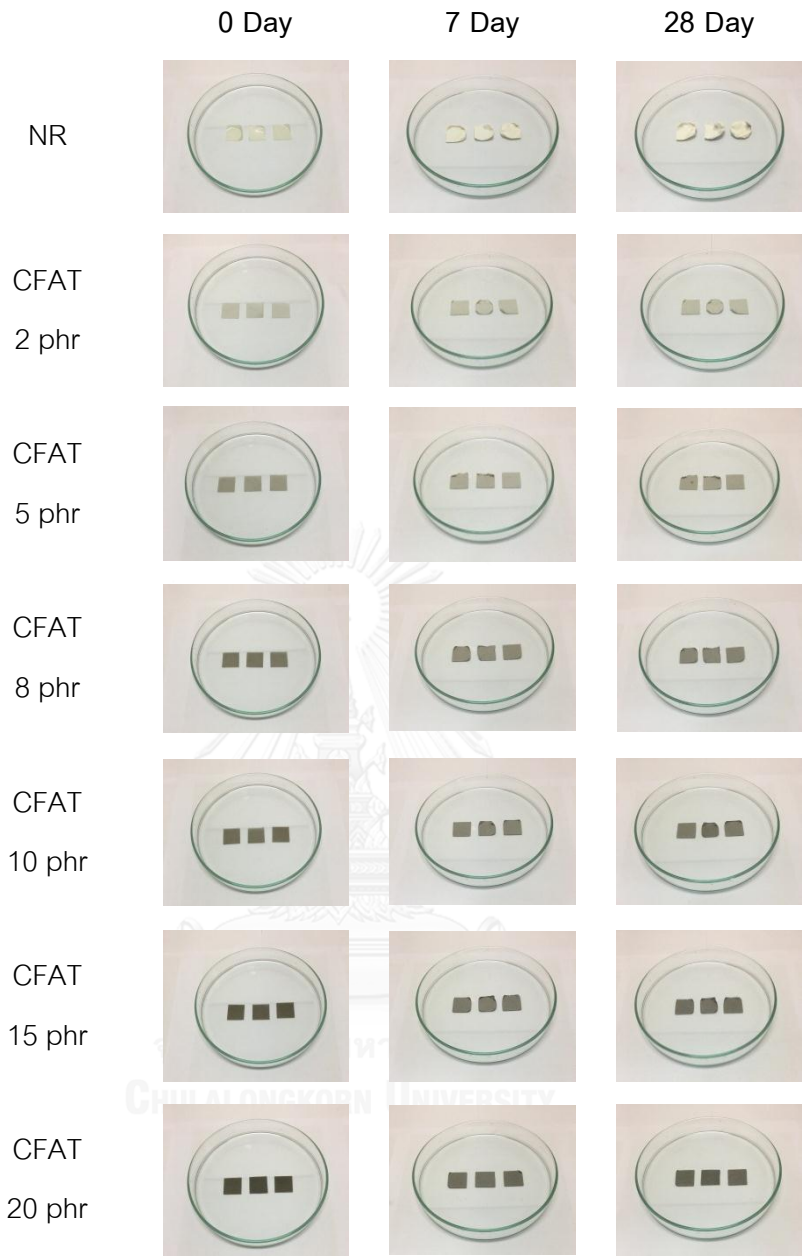

Figure A.2 The swelling behavior in water of NR-CFAT composite films.

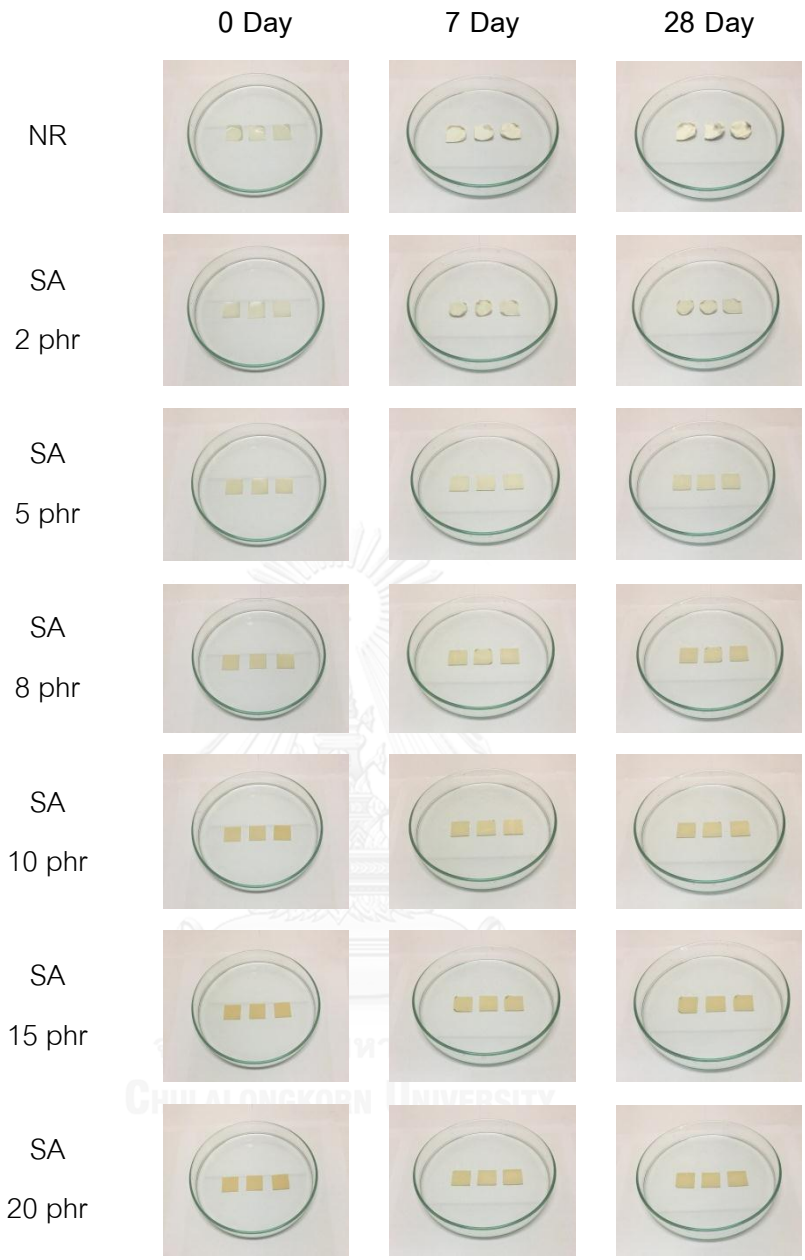

Figure A.3 The swelling behavior in water of NR-SA composite films.

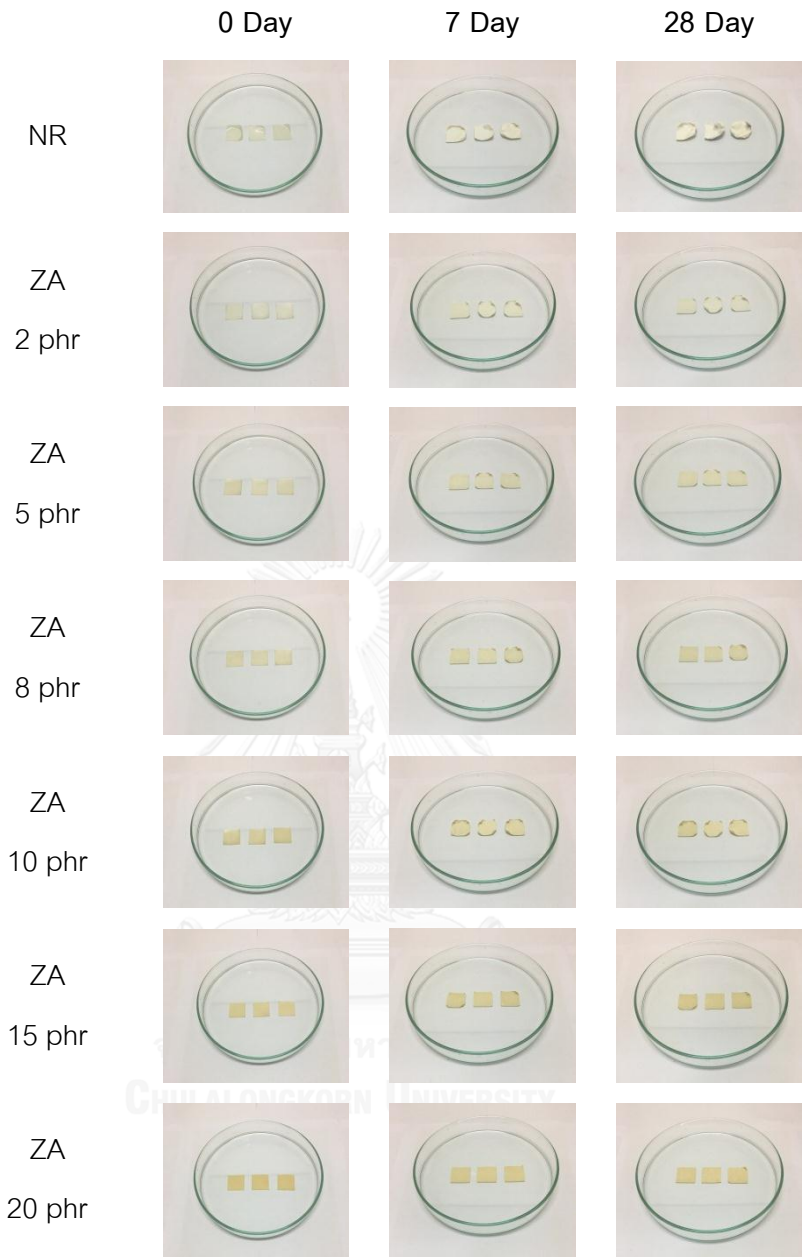

Figure A.4 The swelling behavior in water of NR-ZA composite films.

Table A.2 Data of the weights of the specimen hydrated (W_h) and dried (W_d) of NR and NR-CFA

Samples		W_h(g) 0 Day	W_d (g) 1 Day	3 Day	5 Day	7 Day	14 Day	21 Day	28 Day
NR	1	0.1886	0.2055	0.2180	0.2266	0.2327	0.2439	0.2453	0.2508
	2	0.1779	0.1938	0.2065	0.2148	0.2226	0.2308	0.2331	0.2393
	3	0.1798	0.1954	0.2083	0.2242	0.2242	0.2310	0.2329	0.2376
Average		0.1821	0.1982	0.2109	0.2219	0.2265	0.2352	0.2371	0.2426
CFA2	1	0.0701	0.0706	0.0709	0.0719	0.0705	0.0712	0.0738	0.0722
	2	0.0708	0.0720	0.0715	0.0724	0.0744	0.0732	0.0711	0.0751
	3	0.0760	0.0775	0.0782	0.0765	0.0763	0.0777	0.0773	0.0769
Average		0.0723	0.0734	0.0735	0.0736	0.0737	0.0740	0.0741	0.0747
CFA5	1	0.0964	0.0960	0.0971	0.0973	0.0994	0.0979	0.0963	0.1003
	2	0.0796	0.0792	0.0805	0.0807	0.0813	0.0833	0.0820	0.0833
	3	0.0785	0.0800	0.0787	0.0798	0.0795	0.0791	0.0826	0.0807
Average		0.0848	0.0851	0.0854	0.0859	0.0867	0.0868	0.0870	0.0881
CFA8	1	0.0714	0.0731	0.0720	0.0727	0.0723	0.0745	0.0725	0.0739
	2	0.0715	0.0723	0.0726	0.0733	0.0738	0.0730	0.0763	0.0735
	3	0.0719	0.0722	0.0729	0.0731	0.0742	0.0736	0.0728	0.0744
Average		0.0716	0.0725	0.0725	0.0730	0.0734	0.0737	0.0739	0.0739
CFA10	1	0.0876	0.0897	0.0889	0.0909	0.0938	0.0912	0.0956	0.0933
	2	0.0930	0.0917	0.0904	0.0923	0.0942	0.0954	0.0945	0.0978
	3	0.1048	0.1056	0.1087	0.1054	0.1056	0.1083	0.1091	0.1090
Average		0.0951	0.0957	0.0960	0.0962	0.0979	0.0983	0.0997	0.1000
CFA15	1	0.0744	0.0765	0.0764	0.0758	0.0768	0.0790	0.0802	0.0788
	2	0.0732	0.0735	0.0745	0.0751	0.0747	0.0744	0.0749	0.0743
	3	0.0793	0.0807	0.0823	0.0822	0.0832	0.0819	0.0828	0.0848
Average		0.0756	0.0769	0.0777	0.0777	0.0782	0.0784	0.0793	0.0793
CFA20	1	0.0642	0.0661	0.0674	0.0683	0.0677	0.0705	0.0684	0.0681
	2	0.0726	0.0731	0.0728	0.0732	0.0735	0.0743	0.0751	0.0778
	3	0.0739	0.0743	0.0753	0.0759	0.0789	0.0761	0.0794	0.0772
Average		0.0702	0.0712	0.0718	0.0725	0.0734	0.0736	0.0743	0.0744

Table A.3 Data of the weights of the specimen hydrated (W_h) and dried (W_d) of NR and NR-CFAT

Samples		W_h(g) 0 Day	W_d (g) 1 Day	3 Day	5 Day	7 Day	14 Day	21 Day	28 Day
NR	1	0.1886	0.2055	0.2180	0.2266	0.2327	0.2439	0.2453	0.2508
	2	0.1779	0.1938	0.2065	0.2148	0.2226	0.2308	0.2331	0.2393
	3	0.1798	0.1954	0.2083	0.2242	0.2242	0.2310	0.2329	0.2376
Average		0.1821	0.1982	0.2109	0.2219	0.2265	0.2352	0.2371	0.2426
CFAT2	1	0.0695	0.0706	0.0701	0.0707	0.0713	0.0715	0.0716	0.0733
	2	0.0777	0.0797	0.0816	0.0815	0.0809	0.0804	0.0813	0.0823
	3	0.0730	0.0743	0.0736	0.0739	0.0745	0.0749	0.0741	0.0756
Average		0.0734	0.0749	0.0751	0.0754	0.0756	0.0756	0.0757	0.0771
CFAT5	1	0.0705	0.0715	0.0719	0.0721	0.0726	0.0739	0.0726	0.0728
	2	0.0709	0.0713	0.0722	0.0728	0.0719	0.0721	0.0729	0.0739
	3	0.0699	0.0728	0.0725	0.0727	0.0733	0.0740	0.0747	0.0735
Average		0.0704	0.0719	0.0722	0.0725	0.0726	0.0733	0.0734	0.0734
CFAT8	1	0.0668	0.0697	0.0704	0.0707	0.0693	0.0698	0.0712	0.0716
	2	0.0697	0.0710	0.0719	0.0721	0.0725	0.0732	0.0730	0.0736
	3	0.0694	0.0707	0.0715	0.0711	0.0720	0.0737	0.0732	0.0726
Average		0.0686	0.0705	0.0713	0.0713	0.0713	0.0722	0.0725	0.0726
CFAT10	1	0.0651	0.0659	0.0661	0.0662	0.0657	0.0656	0.0670	0.0665
	2	0.0758	0.0783	0.0781	0.0780	0.0795	0.0792	0.0786	0.0807
	3	0.0770	0.0820	0.0825	0.0833	0.0829	0.0841	0.0836	0.0834
Average		0.0726	0.0754	0.0756	0.0758	0.0760	0.0763	0.0764	0.0769
CFAT15	1	0.0720	0.0742	0.0745	0.0748	0.0759	0.0753	0.0757	0.0764
	2	0.0759	0.0781	0.0785	0.0790	0.0786	0.0795	0.0810	0.0805
	3	0.0743	0.0791	0.0800	0.0797	0.0796	0.0797	0.0788	0.0793
Average		0.0741	0.0771	0.0777	0.0778	0.0780	0.0782	0.0785	0.0787
CFAT20	1	0.0726	0.0782	0.0774	0.0783	0.0785	0.0776	0.0798	0.0777
	2	0.0673	0.0719	0.0731	0.0728	0.0727	0.0733	0.0722	0.0734
	3	0.0684	0.0735	0.0748	0.0742	0.0745	0.0746	0.0736	0.0747
Average		0.0694	0.0745	0.0751	0.0751	0.0752	0.0752	0.0752	0.0753

Table A.4 Data of the weights of the specimen hydrated (W_h) and dried (W_d) of NR and NR-SA

Samples		W_h(g) 0 Day	W_d (g) 1 Day	3 Day	5 Day	7 Day	14 Day	21 Day	28 Day
NR	1	0.1886	0.2055	0.2180	0.2266	0.2327	0.2439	0.2453	0.2508
	2	0.1779	0.1938	0.2065	0.2148	0.2226	0.2308	0.2331	0.2393
	3	0.1798	0.1954	0.2083	0.2242	0.2242	0.2310	0.2329	0.2376
Average		0.1821	0.1982	0.2109	0.2219	0.2265	0.2352	0.2371	0.2426
SA2	1	0.0689	0.0731	0.0738	0.0731	0.0741	0.0743	0.0729	0.0726
	2	0.0668	0.0671	0.0677	0.0694	0.0691	0.0685	0.0702	0.0741
	3	0.0659	0.0678	0.0674	0.0693	0.0699	0.0702	0.0709	0.0680
Average		0.0672	0.0693	0.0696	0.0706	0.0710	0.0710	0.0713	0.0716
SA5	1	0.0837	0.0883	0.0887	0.0902	0.0891	0.0906	0.0894	0.0892
	2	0.0758	0.0794	0.0811	0.0803	0.0802	0.0787	0.0797	0.0809
	3	0.0773	0.0838	0.0825	0.0819	0.0832	0.0836	0.0842	0.0846
Average		0.0789	0.0838	0.0841	0.0841	0.0842	0.0843	0.0844	0.0849
SA8	1	0.0699	0.0729	0.0736	0.0734	0.0734	0.0742	0.0743	0.0748
	2	0.0817	0.0872	0.0881	0.0884	0.0879	0.0884	0.0884	0.0878
	3	0.0861	0.0937	0.0933	0.0936	0.0942	0.0938	0.0942	0.0942
Average		0.0792	0.0846	0.0850	0.0851	0.0852	0.0855	0.0856	0.0856
SA10	1	0.0829	0.0894	0.0887	0.0910	0.0913	0.0921	0.0936	0.0922
	2	0.0694	0.0741	0.0741	0.0737	0.0758	0.0743	0.0734	0.0747
	3	0.0725	0.0775	0.0804	0.0790	0.0778	0.0786	0.0789	0.0790
Average		0.0749	0.0803	0.0811	0.0812	0.0816	0.0817	0.0820	0.0820
SA15	1	0.0723	0.1022	0.1017	0.1018	0.1016	0.1031	0.1021	0.1030
	2	0.0797	0.0746	0.0757	0.0755	0.0751	0.0754	0.0770	0.0767
	3	0.0771	0.0743	0.0736	0.0737	0.0750	0.0753	0.0751	0.0747
Average		0.0764	0.0837	0.0837	0.0837	0.0839	0.0846	0.0847	0.0848
SA20	1	0.0889	0.0739	0.0752	0.0766	0.0770	0.0773	0.0761	0.0778
	2	0.0663	0.0869	0.0879	0.0871	0.0872	0.0872	0.0876	0.0870
	3	0.0655	0.0850	0.0843	0.0844	0.0838	0.0837	0.0852	0.0847
Average		0.0736	0.0819	0.0825	0.0827	0.0827	0.0827	0.0830	0.0832

Table A.5 Data of the weights of the specimen hydrated (W_h) and dried (W_d) of NR and NR-ZA

Samples		W_h(g) 0 Day	W_d (g) 1 Day	3 Day	5 Day	7 Day	14 Day	21 Day	28 Day
NR	1	0.1886	0.2055	0.2180	0.2266	0.2327	0.2439	0.2453	0.2508
	2	0.1779	0.1938	0.2065	0.2148	0.2226	0.2308	0.2331	0.2393
	3	0.1798	0.1954	0.2083	0.2242	0.2242	0.2310	0.2329	0.2376
Average		0.1821	0.1982	0.2109	0.2219	0.2265	0.2352	0.2371	0.2426
ZA2	1	0.0730	0.0773	0.0760	0.0758	0.0767	0.0775	0.0786	0.0782
	2	0.0740	0.0802	0.0776	0.0766	0.0782	0.0785	0.0791	0.0782
	3	0.0736	0.0744	0.0787	0.0802	0.0796	0.0799	0.0784	0.0799
Average		0.0735	0.0773	0.0774	0.0775	0.0782	0.0786	0.0787	0.0788
ZA5	1	0.0729	0.0776	0.0785	0.0790	0.0780	0.0790	0.0794	0.0792
	2	0.0658	0.0702	0.0705	0.0710	0.0704	0.0701	0.0710	0.0710
	3	0.0670	0.0719	0.0710	0.0700	0.0724	0.0721	0.0725	0.0726
Average		0.0686	0.0732	0.0733	0.0733	0.0736	0.0737	0.0743	0.0743
ZA8	1	0.0704	0.0795	0.0799	0.0794	0.0804	0.0789	0.0795	0.0811
	2	0.0882	0.0983	0.0991	0.0992	0.1007	0.1008	0.1012	0.1001
	3	0.0889	0.1008	0.1000	0.1007	0.1004	0.1016	0.1009	0.1013
Average		0.0825	0.0929	0.0930	0.0931	0.0938	0.0938	0.0939	0.0942
ZA10	1	0.0642	0.0705	0.0716	0.0706	0.0723	0.0727	0.0709	0.0727
	2	0.0673	0.0777	0.0782	0.0785	0.0774	0.0768	0.0778	0.0781
	3	0.0669	0.0755	0.0752	0.0766	0.0767	0.0773	0.0781	0.0764
Average		0.0661	0.0746	0.0750	0.0752	0.0755	0.0756	0.0756	0.0757
ZA15	1	0.0725	0.0824	0.0824	0.0830	0.0826	0.0830	0.0831	0.0831
	2	0.0757	0.0874	0.0872	0.0883	0.0879	0.0882	0.0876	0.0883
	3	0.0777	0.0881	0.0897	0.0886	0.0894	0.0898	0.0904	0.0904
Average		0.0753	0.0860	0.0864	0.0866	0.0866	0.0870	0.0870	0.0873
ZA20	1	0.0796	0.0905	0.0919	0.0927	0.0925	0.0930	0.0932	0.0936
	2	0.0709	0.0815	0.0816	0.0810	0.0819	0.0813	0.0814	0.0819
	3	0.0640	0.0752	0.0739	0.0747	0.0749	0.0751	0.0763	0.0763
Average		0.0715	0.0824	0.0825	0.0828	0.0831	0.0831	0.0836	0.0839

Table A.6 Data for Figure 4.12

Samples	Water absorption capacity (%)						
	1 Day	3 Day	5 Day	7 Day	14 Day	21 Day	28 Day
NR	8.86	15.83	21.84	24.38	29.18	30.20	33.21
NRCFA2	1.48	1.71	1.80	1.98	2.40	2.44	3.37
NRCFA5	0.28	0.71	1.30	2.24	2.28	2.51	3.85
NRCFA8	1.30	1.26	2.00	2.56	2.93	3.17	3.26
NRCFA10	0.56	0.91	1.12	2.87	3.33	4.84	5.15
NRCFA15	1.67	2.78	2.73	3.44	3.70	4.85	4.85
NRCFA20	1.33	2.28	3.18	4.46	4.84	5.79	5.89

Table A.7 Data for Figure 4.13

Samples	Water absorption capacity (%)						
	1 Day	3 Day	5 Day	7 Day	14 Day	21 Day	28 Day
NR	8.86	15.83	21.84	24.38	29.18	30.20	33.21
NRCFAT2	2.00	2.32	2.68	2.95	3.00	3.09	5.00
NRCFAT5	2.04	2.51	2.98	3.08	4.12	4.21	4.21
NRCFAT8	2.67	3.84	3.89	3.84	5.25	5.59	5.78
NRCFAT10	3.81	4.04	4.41	4.68	5.05	5.19	5.83
NRCFAT15	4.14	4.86	5.09	5.36	5.54	5.99	6.30
NRCFAT20	7.35	8.16	8.16	8.35	8.26	8.31	8.40

Table A.8 Data for Figure 4.14

Samples	Water absorption capacity (%)						
	1 Day	3 Day	5 Day	7 Day	14 Day	21 Day	28 Day
NR	8.86	15.83	21.84	24.38	29.18	30.20	33.21
NRSA2	3.17	3.62	5.06	5.70	5.65	6.15	6.50
NRSA5	6.21	6.55	6.59	6.63	6.80	6.97	7.56
NRSA8	6.77	7.28	7.45	7.49	7.87	8.08	8.04
NRSA10	7.21	8.19	8.41	8.94	8.99	9.39	9.39
NRSA15	9.60	9.56	9.56	9.86	10.78	10.96	11.04
NRSA20	11.37	12.10	12.42	12.37	12.46	12.78	13.05

Table A.9 Data for Figure 4.15

Samples	Water absorption capacity (%)						
	1 Day	3 Day	5 Day	7 Day	14 Day	21 Day	28 Day
NR	8.86	15.83	21.84	24.38	29.18	30.20	33.21
NRZA2	5.12	5.30	5.44	6.30	6.94	7.03	7.12
NRZA5	6.81	6.95	6.95	7.34	7.54	8.36	8.31
NRZA8	12.57	12.73	12.85	13.74	13.66	13.78	14.14
NRZA10	12.75	13.41	13.76	14.11	14.31	14.31	14.52
NRZA15	14.17	14.79	15.05	15.05	15.54	15.58	15.89
NRZA20	15.24	15.34	15.80	16.22	16.27	16.97	17.39

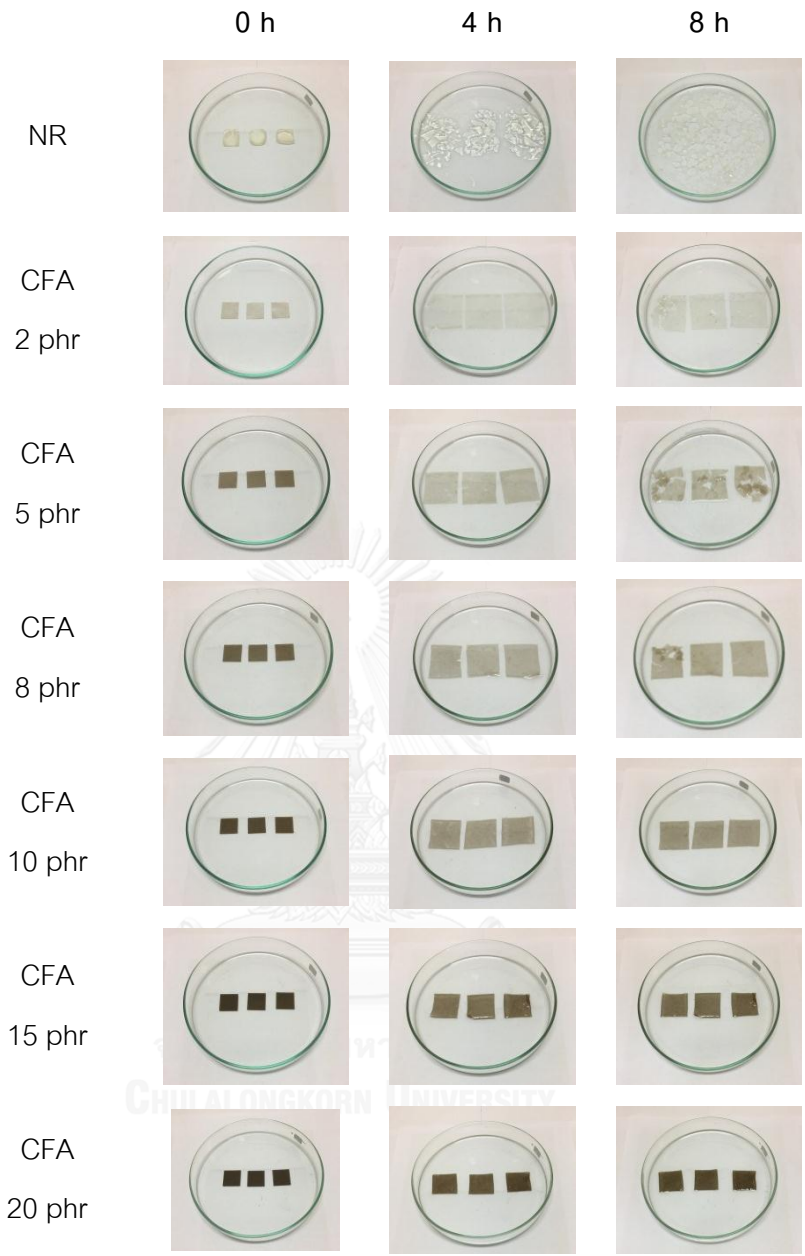

Figure A.5 The swelling behavior in toluene of NR-CFA composite films.

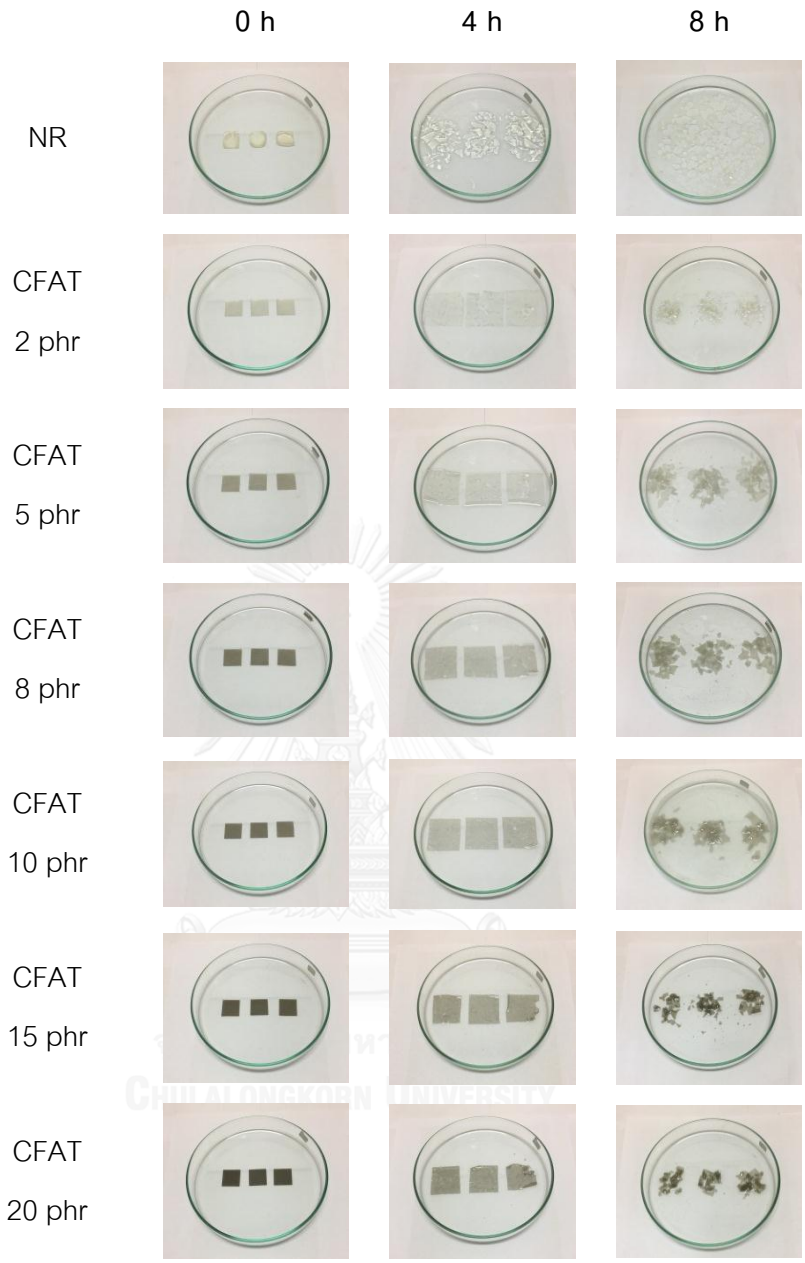

Figure A.6 The swelling behavior in toluene of NR-CFAT composite films.

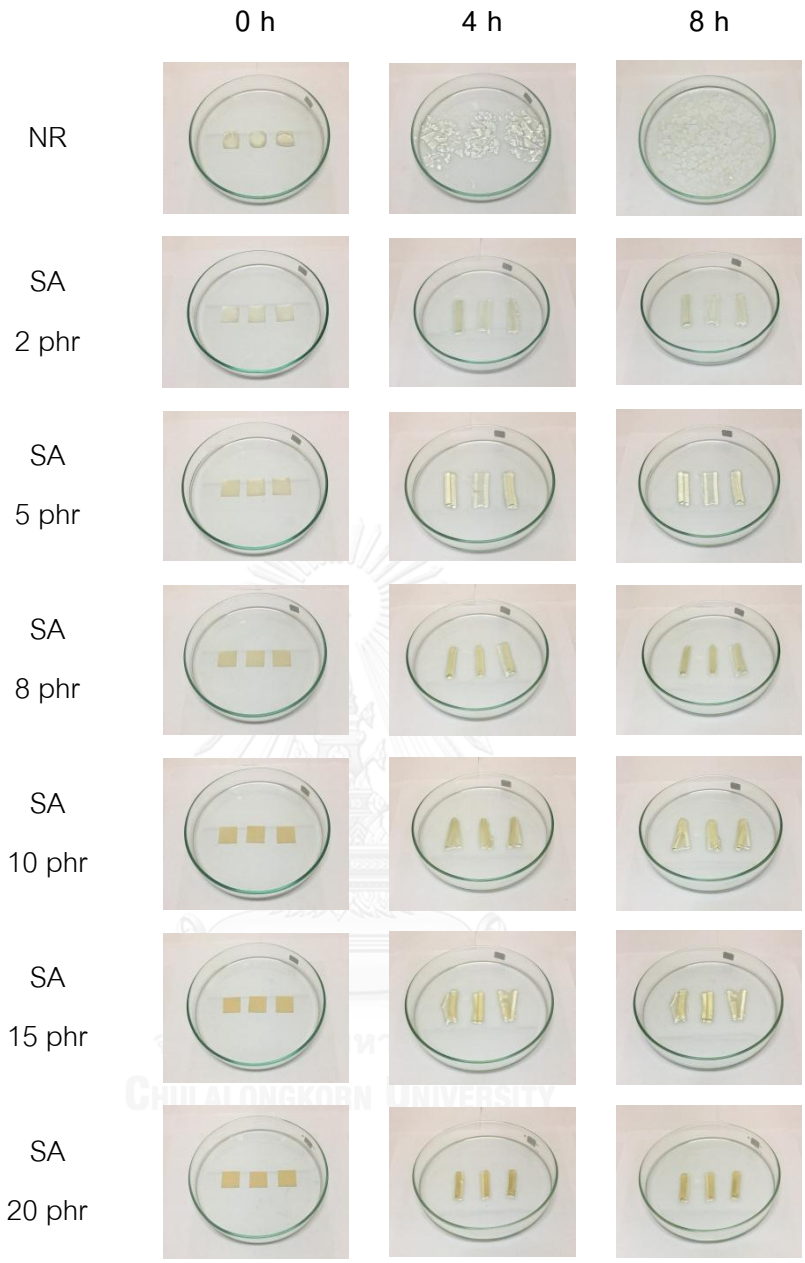

Figure A.7 The swelling behavior in toluene of NR-SA composite films.

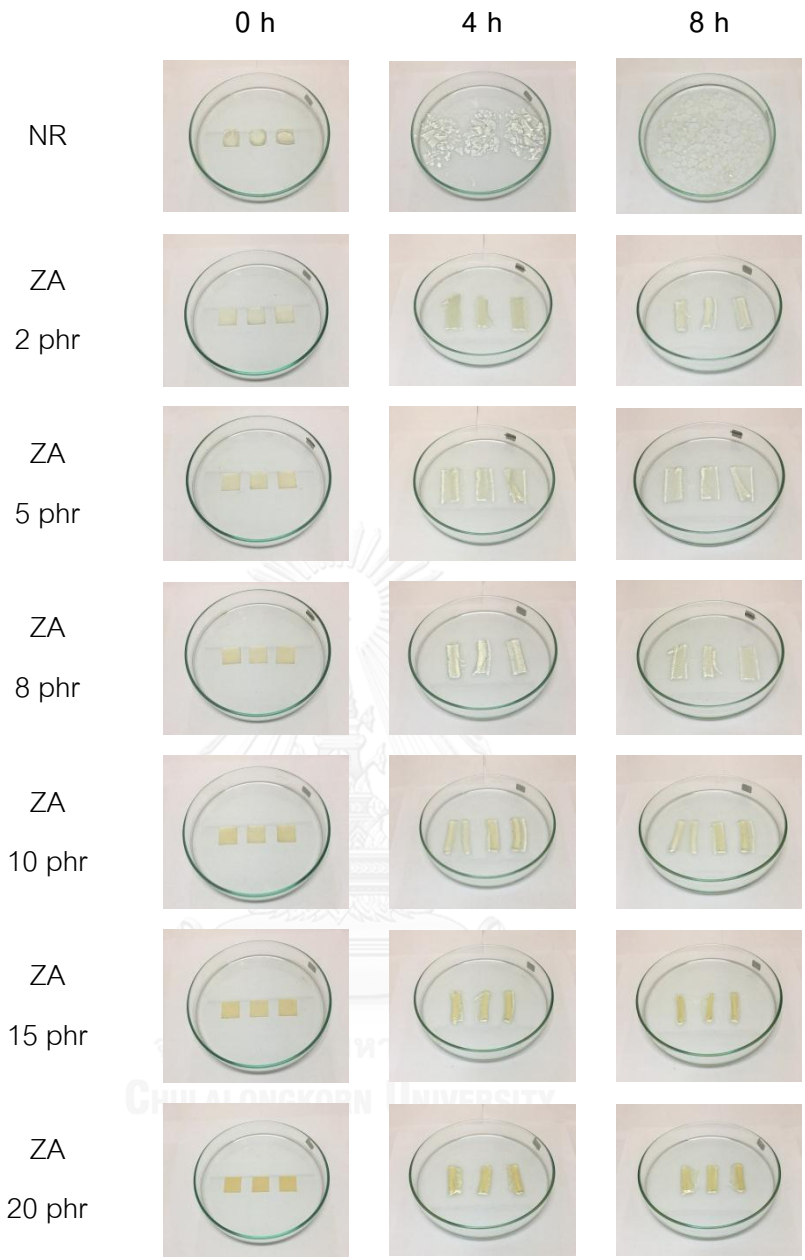

Figure A.8 The swelling behavior in toluene of NR-ZA composite films.

Table A.10 Data of the weights of the specimen before swelling (W_0) and after a time (W_t) of immersion in toluene of NR and NR-CFA

Samples		W_h(g) 0 Day	W_d (g) 1 Day	2 Day	3 Day	4 Day	8 Day
NR	1	0.1596	3.6088	5.5646	3.7529	1.7719	-
	2	0.1582	3.4701	4.5790	3.2116	1.6086	-
	3	0.1402	3.1546	5.0770	3.0685	1.5483	-
Average		0.1527	3.4112	5.0735	3.3443	1.6429	-
CFA2	1	0.0828	0.8763	0.9070	0.8621	0.8610	0.6390
	2	0.0682	0.7713	0.8140	0.7615	0.7758	0.6235
	3	0.0690	0.7754	0.8394	0.8178	0.6471	0.6182
Average		0.0733	0.8077	0.8535	0.8138	0.7613	0.6269
CFA5	1	0.0784	0.7212	0.6920	0.6958	0.6831	0.5735
	2	0.0733	0.7951	0.7394	0.7418	0.6975	0.6487
	3	0.0796	0.8007	0.6954	0.7136	0.7107	0.6034
Average		0.0771	0.7723	0.7089	0.7171	0.6971	0.6085
CFA8	1	0.0730	0.6804	0.6604	0.7502	0.6991	0.5125
	2	0.0721	0.7030	0.6687	0.6957	0.5889	0.5431
	3	0.0711	0.7377	0.6794	0.7056	0.6454	0.5611
Average		0.0721	0.7070	0.6695	0.7172	0.6445	0.5389
CFA10	1	0.0595	0.4718	0.5254	0.5206	0.5176	0.4812
	2	0.0607	0.4328	0.4920	0.4805	0.4871	0.4828
	3	0.0646	0.5361	0.4763	0.4862	0.4855	0.4842
Average		0.0616	0.4802	0.4979	0.4958	0.4967	0.4827
CFA15	1	0.0878	0.6488	0.4754	0.4953	0.5191	0.5046
	2	0.0846	0.4811	0.5075	0.5061	0.5272	0.5137
	3	0.0865	0.4939	0.4802	0.4957	0.5166	0.4981
Average		0.0863	0.5413	0.4877	0.4990	0.5210	0.5055
CFA20	1	0.0750	0.3363	0.3308	0.3331	0.3083	0.3043
	2	0.0736	0.3227	0.3151	0.3161	0.3167	0.3058
	3	0.0743	0.3301	0.3367	0.3373	0.3325	0.3260
Average		0.0743	0.3297	0.3275	0.3288	0.3192	0.3120

Table A.11 Data of the weights of the specimen before swelling (W_0) and after a time (W_t) of immersion in toluene of NR and NR-CFAT

Samples		W_h(g) 0 Day	W_d (g)				
			1 Day	2 Day	3 Day	4 Day	8 Day
NR	1	0.1596	3.6088	5.5646	3.7529	1.7719	-
	2	0.1582	3.4701	4.5790	3.2116	1.6086	-
	3	0.1402	3.1546	5.0770	3.0685	1.5483	-
Average		0.1527	3.4112	5.0735	3.3443	1.6429	-
CFAT2	1	0.0681	0.8173	0.9105	0.8469	0.8069	-
	2	0.0720	0.8869	0.7986	0.8150	0.7841	-
	3	0.0644	0.7466	0.7931	0.8281	0.8362	-
Average		0.0682	0.8169	0.8341	0.8300	0.8091	-
CFAT5	1	0.0743	0.8168	0.8973	0.7836	0.7571	-
	2	0.0728	0.8226	0.9092	0.8582	0.7728	-
	3	0.0741	0.8618	0.8981	0.8103	0.6974	-
Average		0.0737	0.8337	0.9015	0.8174	0.7424	-
CFAT8	1	0.0677	0.7482	0.7682	0.7740	0.7244	-
	2	0.0723	0.7989	0.7169	0.7672	0.6265	-
	3	0.0705	0.7214	0.7215	0.7421	0.7461	-
Average		0.0702	0.7562	0.7355	0.7611	0.6990	-
CFAT10	1	0.0754	0.7331	0.7307	0.6723	0.6268	-
	2	0.0801	0.8021	0.7091	0.7218	0.7452	-
	3	0.0757	0.7480	0.7782	0.7784	0.7336	-
Average		0.0771	0.7611	0.7393	0.7242	0.7019	-
CFAT15	1	0.0709	0.7106	0.6766	0.6311	0.5516	-
	2	0.0688	0.7085	0.5738	0.6267	0.5702	-
	3	0.0706	0.7194	0.6374	0.6228	0.5751	-
Average		0.0701	0.7128	0.6293	0.6269	0.5656	-
CFAT20	1	0.0750	0.6919	0.5933	0.5772	0.5283	-
	2	0.0693	0.7117	0.5863	0.4698	0.4425	-
	3	0.0870	0.5954	0.5452	0.4991	0.4784	-
Average		0.0771	0.6663	0.5749	0.5154	0.4831	-

Table A.12 Data of the weights of the specimen before swelling (W_0) and after a time (W_t) of immersion in toluene of NR and NR-SA

Samples		W_h(g) 0 Day	W_d (g)				
			1 Day	2 Day	3 Day	4 Day	8 Day
NR	1	0.1596	3.6088	5.5646	3.7529	1.7719	-
	2	0.1582	3.4701	4.5790	3.2116	1.6086	-
	3	0.1402	3.1546	5.0770	3.0685	1.5483	-
Average		0.1527	3.4112	5.0735	3.3443	1.6429	-
SA2	1	0.0643	0.7630	0.8853	0.8335	0.7584	0.7158
	2	0.0661	0.8095	0.7098	0.7819	0.8468	0.8084
	3	0.0721	0.8745	0.7793	0.8054	0.7845	0.8012
Average		0.0675	0.8157	0.7915	0.8069	0.7966	0.7751
SA5	1	0.0763	0.8815	0.8959	0.8964	0.9018	0.8387
	2	0.0775	0.8911	0.8655	0.8538	0.8472	0.8836
	3	0.0743	0.8741	0.8774	0.8378	0.8232	0.8113
Average		0.0760	0.8822	0.8796	0.8627	0.8574	0.8445
SA8	1	0.0785	0.7608	0.7651	0.7564	0.7285	0.7326
	2	0.0805	0.7378	0.7087	0.7323	0.7721	0.7224
	3	0.0821	0.7626	0.7445	0.7159	0.7287	0.7508
Average		0.0804	0.7537	0.7394	0.7349	0.7431	0.7353
SA10	1	0.0702	0.5891	0.6276	0.5658	0.5711	0.5635
	2	0.0786	0.6533	0.5590	0.6344	0.6479	0.6011
	3	0.0764	0.5810	0.5493	0.6278	0.6332	0.6485
Average		0.0751	0.6078	0.5786	0.6093	0.6174	0.6044
SA15	1	0.0664	0.5434	0.5966	0.5489	0.5015	0.5139
	2	0.0783	0.4869	0.5025	0.5113	0.5322	0.4701
	3	0.0715	0.5030	0.4823	0.4669	0.4751	0.5183
Average		0.0721	0.5111	0.5271	0.5090	0.5029	0.5008
SA20	1	0.0894	0.5437	0.5809	0.5765	0.5983	0.5788
	2	0.0806	0.6069	0.6351	0.6101	0.5957	0.5540
	3	0.0814	0.5546	0.5610	0.6632	0.6325	0.5631
Average		0.0838	0.5684	0.5923	0.6166	0.6088	0.5653

Table A.13 Data of the weights of the specimen before swelling (W_0) and after a time (W_t) of immersion in toluene of NR and NR-ZA

Samples		W_h(g) 0 Day	W_d (g) 1 Day	2 Day	3 Day	4 Day	8 Day
NR	1	0.1596	3.6088	5.5646	3.7529	1.7719	-
	2	0.1582	3.4701	4.5790	3.2116	1.6086	-
	3	0.1402	3.1546	5.0770	3.0685	1.5483	-
Average		0.1527	3.4112	5.0735	3.3443	1.6429	-
ZA2	1	0.0748	0.8882	1.1140	0.9598	0.8979	0.8361
	2	0.0693	0.9917	1.1264	1.1557	0.8703	0.9147
	3	0.0719	1.0273	1.0472	1.0746	0.8374	0.8724
Average		0.0720	0.9691	1.0959	1.0634	0.8685	0.8744
ZA5	1	0.0777	0.8368	0.8442	0.8637	0.7188	0.7829
	2	0.0681	0.8255	0.8723	0.8974	0.8534	0.8150
	3	0.0738	0.8582	0.8804	0.7491	0.8709	0.7974
Average		0.0732	0.8402	0.8656	0.8367	0.8144	0.7984
ZA8	1	0.0716	0.8212	0.8449	0.8566	0.8818	0.8852
	2	0.0711	0.7670	0.8076	0.8604	0.8073	0.7378
	3	0.0674	0.6526	0.8612	0.8021	0.7745	0.8489
Average		0.0700	0.7469	0.8379	0.8397	0.8212	0.8240
ZA10	1	0.0694	0.8568	0.8989	0.8861	0.8752	0.8549
	2	0.0802	0.7758	0.8974	0.8622	0.9083	0.8743
	3	0.0847	0.7247	0.8705	0.8997	0.8826	0.8528
Average		0.0781	0.7858	0.8889	0.8827	0.8887	0.8607
ZA15	1	0.0653	0.5043	0.5526	0.5539	0.5388	0.5221
	2	0.0642	0.5384	0.5414	0.5584	0.5233	0.5508
	3	0.0641	0.4841	0.5138	0.4923	0.5585	0.5076
Average		0.0645	0.5089	0.5359	0.5349	0.5402	0.5268
ZA20	1	0.0786	0.5012	0.5384	0.5412	0.5416	0.5474
	2	0.0786	0.4874	0.5369	0.5298	0.5429	0.5410
	3	0.0785	0.4839	0.5325	0.5475	0.5469	0.5457
Average		0.0786	0.4908	0.5359	0.5395	0.5438	0.5447

Table A.14 Data for Figure 4.16

Samples	Toluene uptake (%)				
	1 h	2 h	3 h	4 h	8 h
NR	2134.39	3223.28	2090.61	976.16	-
NRCFA2	1001.36	1063.82	1009.73	938.14	754.86
NRCFA5	901.73	819.50	830.05	804.15	689.28
NRCFA8	881.08	829.00	895.14	794.26	647.78
NRCFA10	679.60	708.28	704.82	706.39	683.66
NRCFA15	527.19	465.12	478.25	503.67	485.71
NRCFA20	343.74	340.83	342.58	329.56	319.96

Table A.15 Data for Figure 4.17

Samples	Toluene uptake (%)				
	1 h	2 h	3 h	4 h	8 h
NR	2134.39	3223.28	2090.61	976.16	-
NRCFAT2	1098.44	1123.57	1117.60	1086.89	-
NRCFAT5	1030.74	1122.69	1008.54	906.92	-
NRCFAT8	977.67	948.27	984.70	896.20	-
NRCFAT10	887.54	859.34	839.66	810.73	-
NRCFAT15	916.88	797.67	794.25	706.89	-
NRCFAT20	764.25	645.70	568.44	526.55	-

Table A.16 Data for Figure 4.18

Samples	Toluene uptake (%)				
	1 h	2 h	3 h	4 h	8 h
NR	2134.39	3223.28	2090.61	976.16	-
NRSA2	1108.40	1072.54	1095.46	1080.10	1048.35
NRSA5	1060.32	1056.86	1034.59	1027.66	1010.74
NRSA8	837.87	820.07	814.39	824.64	814.89
NRSA10	709.68	670.83	711.72	722.47	705.11
NRSA15	609.20	631.45	606.34	597.87	594.87
NRSA20	578.28	606.84	635.80	626.53	574.58

Table A.17 Data for Figure 4.19

Samples	Toluene uptake (%)				
	1 h	2 h	3 h	4 h	8 h
NR	2134.39	3223.28	2090.61	976.16	-
NRZA2	1245.93	1422.04	1376.90	1106.30	1114.44
NRZA5	1047.77	1082.56	1043.08	1012.52	990.76
NRZA8	966.54	1096.43	1099.00	1072.58	1076.53
NRZA10	906.10	1038.20	1030.17	1037.90	1002.01
NRZA15	688.64	730.48	728.82	737.09	716.37
NRZA20	524.73	582.14	586.68	592.15	593.30

VITA

Miss Jaygita Wikranvanich was born on January 11,1992 in Bangkok, Thailand. She graduated with Bachelor's degree of Engineering from the Department of Chemical Engineering, Mahidol University in 2014. She continued studying Master's degree of Chemical Engineering in Biochemical Research Group at Chulalongkorn University and finished her study in December 2016.

Presentation in Conference:

July 2016: Poster presentation in 6th International Polymer Conference of Thailand (PCT-6). Pathumwan Princess Hotel, Bangkok, Thailand